Studies of Vibrational Surface Modes. II. Monatomic fcc Crystals*

R. E. Allen,† G. P. Alldredge, and F. W. de Wette
Department of Physics, University of Texas, Austin, Texas 78712
(Received 1 March 1971)

We report the first thorough study of vibrational surface modes in realistic crystal models. This study was based on calculations for monatomic fcc crystals with (111), (100), and (110) surfaces. The most important general result is the following: In addition to the class of surface-mode branches that persist into the long-wavelength limit, studied extensively by previous workers, there is a second class of surface modes that exist only at relatively small wavelengths (of the order of an atomic spacing). The existence of such modes was pointed out in two earlier publications, but a detailed examination of the properties of these modes is presented in the present paper. For the (111) surface, there are five distinct surface-mode branches; for the (100) surface there are apparently at least 19; and for the (110) surface there are ten. A number of series of mixed (or pseudosurface) modes have also been identified. Many of the surface modes are primarily localized in the second layer beneath the surface or some deeper layer, rather than the surface layer itself. At some symmetry points, modes are obtained in which a single layer vibrates almost independently. Several cases have been found in which surface-mode branches attempt to cross each other and as a result exhibit hybridization. The surface modes and mixed modes have been studied throughout the interior of the two-dimensional Brillouin zone, as well as along the symmetry lines. The dispersion curves are shown, graphs are given for the attenuation of many of the modes with distance from the surface, and the polarizations of the modes are described. The behavior of the modes with respect to uniform changes in the density and changes in the surface force constants has been investigated: In all cases the Grüneisen parameters for surface modes and bulk modes are approximately the same for uniform changes in density. If the surface force constants are increased by neglecting the relaxation of the surface particles, the surface-mode frequencies are increased, as one expects. In some cases, these frequencies are raised into the bulk continua and the modes become delocalized. This fact implies that the surface relaxation is important, and the qualitative features of the surface-mode spectrum are sensitive to changes in the surface force constants. Although the calculated surface-mode spectra are rather complicated, all of the surface modes and mixed modes can be explained in terms of a simple phenomenological model in which these modes are regarded as "peeling off" from the bulk bands in a systematic fashion: A mode which is primarily localized in the first layer peels off first from a given bulk band, then (if the perturbation due to the surface is strong enough) a second mode which is primarily localized in the second layer peels off, etc., with the nth-layer mode having the same character in the nth layer as the first-layer mode has in the first layer.

I. INTRODUCTION

In the preceding paper[1] we gave a formal treatment of the lattice-dynamics problem for an arbitrary crystal with two-dimensional periodicity and one or two surfaces. In this paper we will present the results of detailed numerical calculations for monatomic fcc crystals with (111), (100), and (110) surfaces. Some of these results have been briefly described in previous publications.[2,3]

The work of this paper is part of a program to study the vibrational properties of realistic model crystals with surfaces. As discussed in I, the model used in the present work is a slab-shaped crystal of finite thickness in which the particles interact through a Lennard-Jones potential. The justification for using this model, the motivation for studying vibrational surface properties, and a description of the previous work in this area have been given elsewhere.[1,4]

In Sec. II of the present paper, we discuss the relationship between the vibrational modes in a crystal with two parallel surfaces and those in a crystal with three-dimensional periodic boundary conditions. It is pointed out that there can be gaps within the bulk subbands[5] for a crystal with surfaces, and that surface modes can exist within these gaps. In Secs. III and IV, the calculated surface-mode spectra for the (111), (100), and (110) surfaces are presented and discussed. It is found that these spectra are surprisingly complex. In addition to the usual generalized Rayleigh waves, which exist in the long-wavelength limit, there are many other surface modes which exist only for relatively small wavelengths. In Sec. V, it is shown how the surface-mode spectra, despite their complexity, can be interpreted in terms of a very simple model. In Sec. VI, the effects of changes in the surface

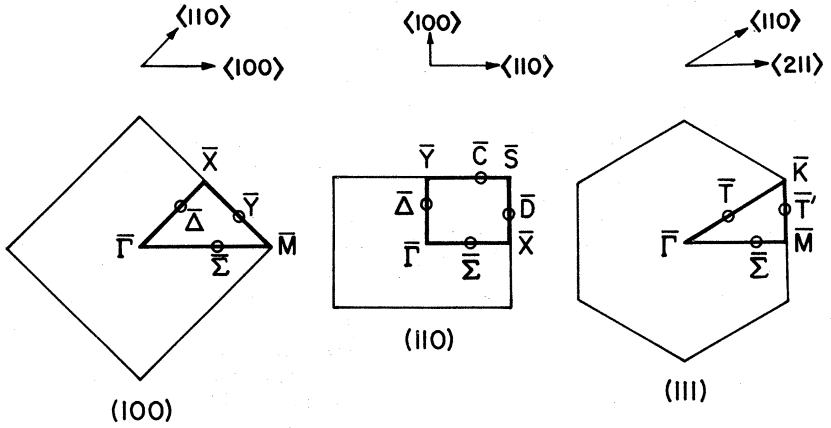

FIG. 1. BZ's for the (100), (110), and (111) surfaces of an fcc crystal.

force constants and the density are examined. It is found that the surface relaxation must be taken into account in order to obtain the correct qualitative features of the surface-mode spectra. In Sec. VII, results for the surface frequency distribution function $f^s(\omega)$ and an "effective frequency distribution function" $f_\alpha(\omega; l_3)$ are presented and discussed. Finally, in Sec. VIII the main conclusions of the preceding sections are summarized.

II. MODES OF VIBRATION IN A SLAB

As discussed in I, the normal-mode solutions for a crystal with two parallel surfaces have the form

$$u_\alpha(\vec{l}) = u_\alpha(l_3)\, e^{i(\bar{q}\cdot\bar{r}_0^{\bar{l}} - \omega t)} \tag{2.1}$$

when there is one particle per unit cell. Here $\bar{q} = (q_x, q_y)$ is the two-dimensional propagation vector and the other symbols are defined in I. Distinct solutions correspond to values of $\bar{q}$ lying within the first two-dimensional Brillouin zone (BZ), which is determined by the crystal structure and the surface orientation. The modes in the whole BZ are

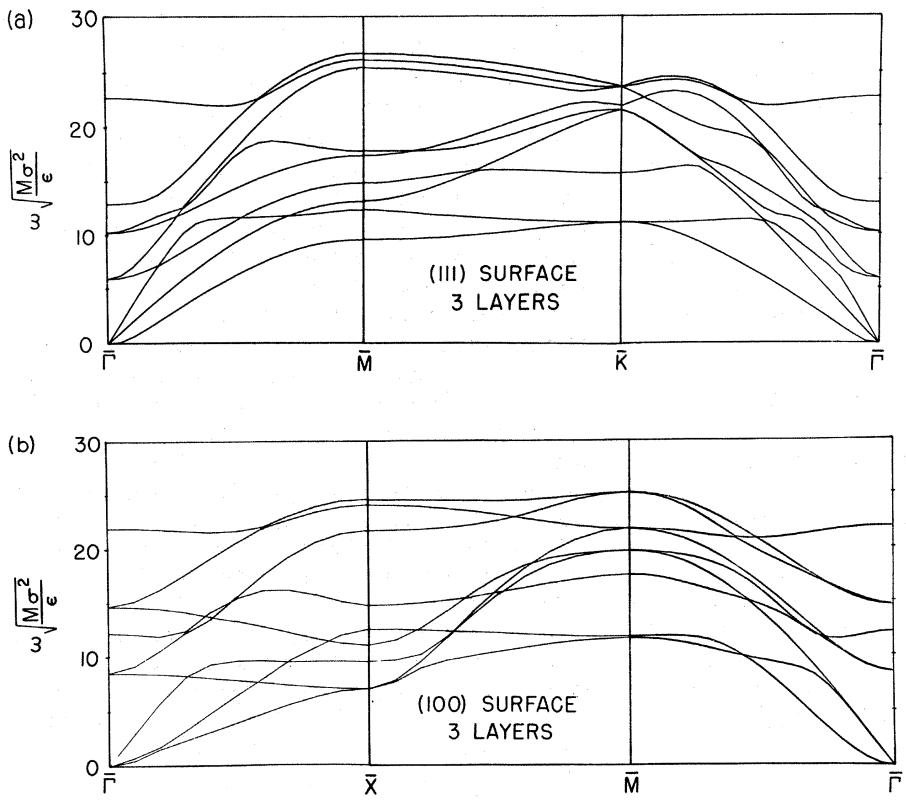

FIG. 2. (a) Frequency ω vs two-dimensional wave vector $\bar{q}$, for $\bar{q}$ lying along symmetry lines $\bar{\Gamma}\bar{M}$ and $\bar{K}\bar{\Gamma}$ and BZ edge $\bar{M}\bar{K}$, in the case of a three-layer slab with (111) surfaces. M is the mass of a particle and ϵ and σ are the Lennard-Jones potential parameters. [See Eq. (1.3) of I.] (b) ω vs $\bar{q}$ for three-layer slab with (100) surfaces.

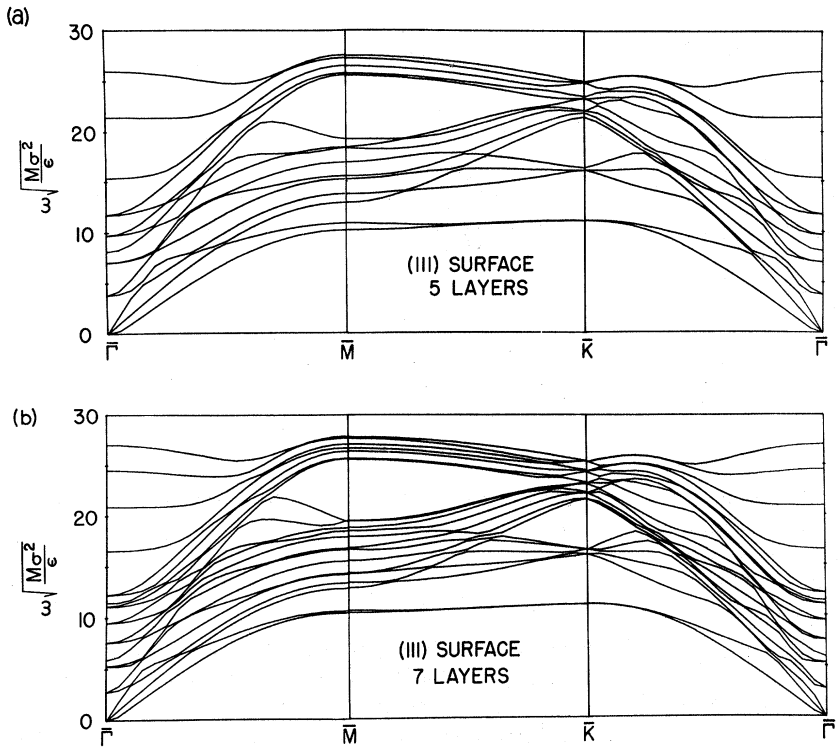

FIG. 3. ω vs $\bar{q}$ for (a) five- and (b) seven-layer slabs with (111) surfaces. There are, respectively, $3\times5=15$ and $3\times7=21$ branches. These curves were computer generated; in this figure, and all the similar figures that follow, no attempt was made to reconnect the curves properly when crossovers between modes occur within the bulk bands. (These crossovers are not of interest because we are here concerned with surface modes.) Also, the length of the horizontal lines in these figures is taken to be the same for different symmetry lines (e.g., $\bar{\Gamma}\bar{M}$ and $\bar{M}\bar{K}$) rather than proportional to the length of the symmetry lines as shown in Fig. 1.

determined by those in the irreducible element (IE) through simple symmetry transformations. In Fig. 1, the BZ's for the (100), (110), and (111) surfaces of an fcc crystal are shown, with the IE in each case surrounded by heavy lines. The scheme which we will use for labeling the symmetry points is indicated (see also Fig. 1 of I), and the crystallographic directions associated with the symmetry lines are given. Most of the calculations reported in this paper are for values of $\bar{q}$ lying along the boundaries of the IE (heavy lines of Fig. 1), since the behavior of the modes along these boundaries provides a good indication of the behavior within the rest of the IE. We have, however, studied the modes throughout the IE in detail for each surface, and some results will be given for values of $\bar{q}$ lying in the interior of the IE.

The normal-mode frequencies are obtained by numerically solving the eigenvalue equation

$$\sum_{l_3'\beta} D_{\alpha\beta}(l_3 l_3'; \bar{q})\xi_\beta(l_3'; \bar{q}p) = \omega_p^2(\bar{q})\xi_\alpha(l_3; \bar{q}p) \qquad (2.2)$$

[see Eq. (2.25) of I]. There are $3N_3$ frequencies $\omega_p(\bar{q})$ for each wave vector $\bar{q}$, where N_3 is the number of layers in the slab-shaped crystal. In Fig. 2, we show $\omega_p(\bar{q})$-vs-$\bar{q}$ graphs for slabs with only three planes of particles which have (111) and (100) surfaces, respectively. Since $N_3=3$, there are $3\times3=9$ frequencies for each $\bar{q}$. The incipiency of both the bulk bands and the curves corresponding to low-frequency surface modes can already be seen in crystals this thin. [Compare Fig. 2(a) with Fig. 8 and Fig. 2(b) with Fig. 10.]

In Fig. 3, the ω-vs-$\bar{q}$ curves for five- and seven-layer slabs with (111) surfaces are shown. It is evident that, as the thickness increases, the bulk bands fill up and there is a rapid decrease in the splitting between the curves corresponding to surface modes of the same kind[6] (see, e.g., the lowest-frequency surface mode at the point $\bar{M}$). (As discussed in Sec. IIIC of I, a single surface mode in a semi-infinite crystal gives rise to a pair of surface modes in a slab, with the degeneracy of the pair broken by the finite thickness of the slab.) The results for an 11-layer slab are shown in Ref. 2, and the results for 21 layers are shown in Fig. 8 of this paper. For the 21-layer slab, the surface-mode branches (discrete states) are clearly separated from the bulk "bands" (quasicontinuum of states in a semi-infinite crystal). This thickness was also found to be adequate for the (100) and (110) surfaces. We have therefore used 21-layer models in performing the calculations whose results are given in Secs. III, IV, and VI.

It is apparent in Fig. 3 that there are gaps in the bulk bands near the edge of the Brillouin zone. One can get an idea how these gaps, and the general structure of the bulk bands, arise by examining the relationship between the modes in the slab with two free surfaces and those in another slab which has the same structure and the same thick-

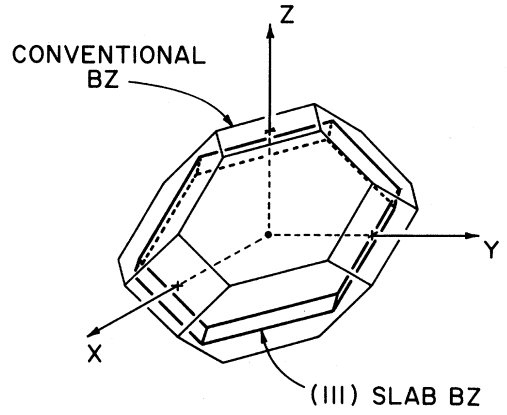

FIG. 4. Conventional BZ and "slab-adapted" BZ for the (111) surface.

ness, but for which periodic boundary conditions are applied in the z direction. In the case of the first slab, there will be surface modes and mixed modes in addition to the bulk modes. In the case of the second slab, all of the modes will be bulk modes, since there are no surfaces. The "severing" of the periodic boundary conditions to obtain the first slab from the second one can be regarded as a (strong) perturbation which alters the vibrational modes, and in fact converts some of them into surface modes and mixed modes.[7]

In the slab with three-dimensional periodic boundary conditions, the three-dimensional translational invariance implies that each normal-mode solution has a well-defined (and real) three-dimensional propagation vector $\vec{q} = (q_x, q_y, q_z)$. The distinct solutions correspond to values of $\vec{q}$ that can be chosen to lie in a nonprimitive three-dimensional BZ, which will be called the "slab-adapted" BZ. This BZ is not the same as the usual BZ for an fcc crystal, since our choice of fundamental lattice vectors for the slab is not the same as the usual choice for an fcc crystal (see Sec. II of I).

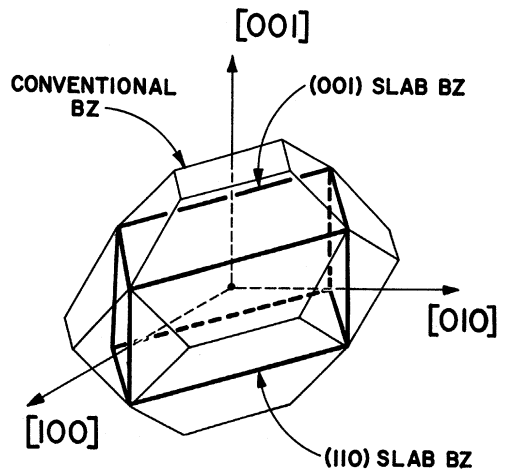

FIG. 5. Slab-adapted BZ's for (110) and (001) surfaces. The BZ for the (100) surface is, of course, identical in shape to that for the (001) surface, but is less convenient to display.

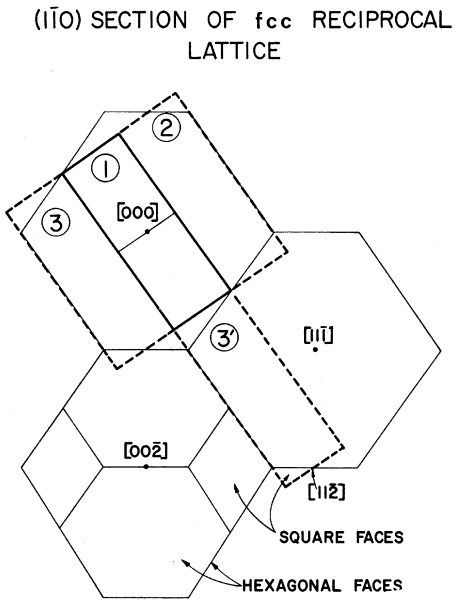

FIG. 6. (1$\bar{1}$0) cross section of the first three-dimensional BZ and the nearby region of reciprocal space.

In Figs. 4 and 5 we show the "slab-adapted" BZ's which are appropriate for the surfaces studied in this paper—namely, the (111), (100), and (110) surfaces. For comparison, we also show the conventional (primitive) BZ for an fcc crystal. In the case of the (111) surface, the $(n+3)$th plane in the slab is equivalent to the nth plane. There are thus three particles per unit cell in the slab, as compared with one particle per unit cell for the usual choice of primitive translation vectors, and the slab-adapted BZ consequently has one-third the volume of the conventional BZ. In the case of the (100) or (110) surface, the $(n+2)$th plane in the slab is equivalent to the nth plane. There are thus two particles per unit cell in the slab, and the slab-adapted BZ has one-half the volume of the conventional BZ.

One can remap the normal modes for the conventional BZ (one particle per unit cell) into the slab-adapted BZ (two or three particles per unit cell). As an example, we will explicitly show how such a remapping proceeds in the case of the (111) surface. In Fig. 6, a (1$\bar{1}$0) cross section is shown of three-dimensional reciprocal space. The six-sided figure centered at the origin is the cross section of the conventional first BZ. One can show that this BZ

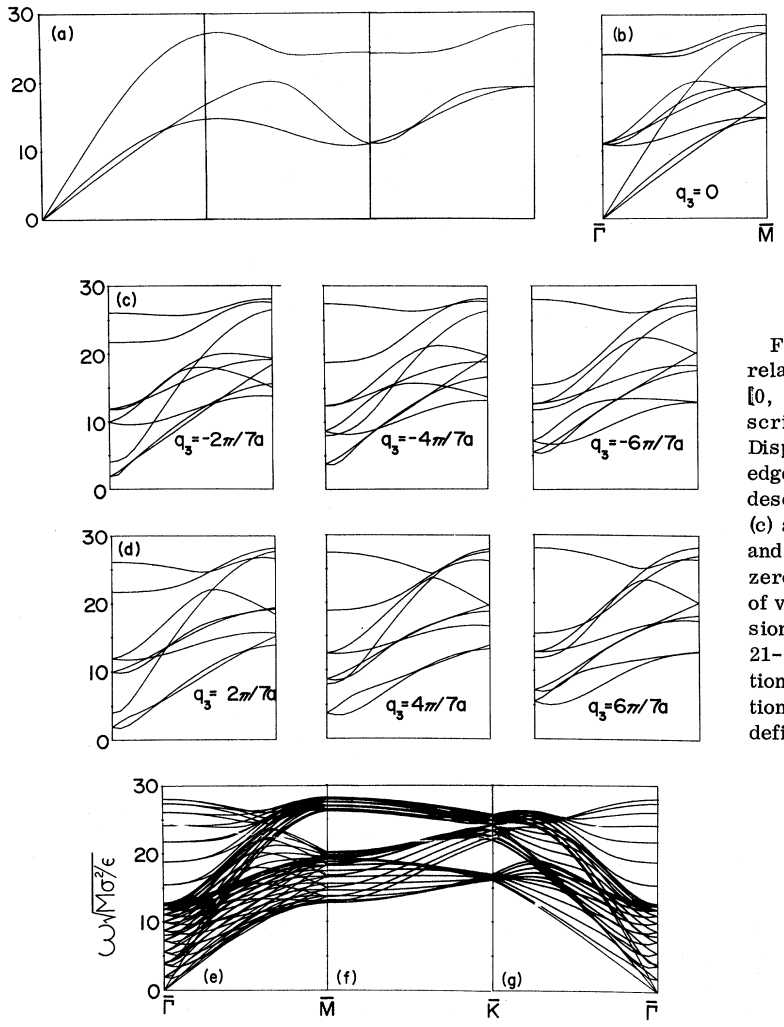

FIG. 7. (a) Dispersion curves (ω vs $\vec{q}$ relations) along the line between the points [0, 0, 0] and [1, 1, $\bar{2}$] of Fig. 6, in the description with one particle per unit cell. (b) Dispersion curves between the origin and the edge of the slab-adapted BZ for $q_z = 0$, in the description with three particles per unit cell. (c) and (d) ω vs $\vec{q}$ relations between the origin and the edge of the slab-adapted BZ for nonzero values of q_z. (e), (f), and (g) Dependence of vibrational frequencies on the two-dimensional propagation vector $\bar{q} = (q_x, q_y)$ for a 21-layer slab with periodic boundary conditions in the z direction. (e) is a superposition of (b)–(d). The points $\bar{\Gamma}$, $\bar{M}$, and $\bar{K}$ are defined in Fig. 1.

can be mapped into a volume consisting of three hexagonal slabs, whose cross sections are labeled by the encircled numbers 1, 2, and 3 in Fig. 6; i.e., the pieces that lie within the hexagonal slabs and not within the conventional BZ are obtained from the pieces that lie within the conventional BZ and not within the slabs by translating the latter through reciprocal lattice vectors (of the nonprimitive lattice). There is consequently a one-to-one correspondence between the normal-mode solutions for values of $\vec{q}$ lying in the conventional BZ and those for values of $\vec{q}$ lying in the hexagonal region.

In the description with three particles per unit cell, the values of $\vec{q}$ are limited to the hexagonal slab labeled "1" (which is the same as the slab shown in Fig. 4). The modes for a given value of $\vec{q}$ in this description correspond to the modes for three values of $\vec{q}$ in the description with one particle per unit cell, one value lying in each of the three hexagonal slabs labeled "1," "2," and "3."

In Fig. 7 we show one way in which the normal-mode frequencies can be obtained for the slab-adapted BZ. In Fig. 7(a), the $\omega(\vec{q})$-vs-$\vec{q}$ curves are shown for $\vec{q}$ lying on a straight line between the points [0, 0, 0] and [1, 1, $\bar{2}$], in the notation of Fig. 6. The first third of this line lies in the slab labeled "1" and the last third in the slab labeled "3′," which is equivalent to the one labeled "3." The middle section of the line lies in "3′" also, but it is equivalent to a line lying in "2" (with the direction reversed), because of the inversion symmetry evident in Fig. 6. When the frequencies in Fig. 7(a) are appropriately remapped from slabs "1," "2," and "3" into slab "1," we obtain the curve in Fig. 7(b).

The results shown in Fig. 7(b) correspond to $q_z = 0$, where the z axis is now taken to be perpendicular to the planes of the slab—i.e., in the [111] direction according to the notation of Fig. 6. In the succeeding frames we show results which were similarly obtained for other values of q_z lying between the top and the bottom of the slab-adapted

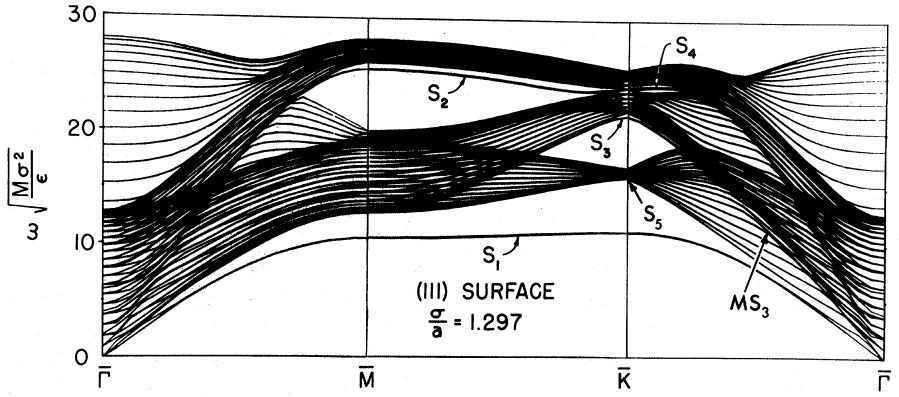

FIG. 8. ω vs $\bar{q}$ for a 21-layer slab with (111) surfaces. Here a is one-half the lattice spacing, so that $\sqrt{2}\,a$ is the nearest-neighbor distance; $\sigma/a = 1.297$ corresponds to the density of a static crystal. The lines marked $S_i (i = 1, 2, 3, 4, 5)$ correspond to surface-mode branches in a semi-infinite crystal. In a slab with two surfaces, there are actually two nearly degenerate modes corresponding to each surface mode in semi-infinite crystal, so the lines in this figure are actually double lines. Ordinarily the two lines nearly coincide, but for S_1 near the origin ($\bar{\Gamma}$), the penetration depth becomes large, the degeneracy is broken, and the lines separate. In addition to the five distinct surface-mode branches, there is a series of mixed modes MS_3 which can be seen as a disturbance in the lowest bulk band along $\bar{K}\bar{\Gamma}$.

BZ. These values of q_z, including $q_z = 0$, are the values appropriate to a slab-shaped crystal which is 21 layers thick. (Recall that a unit cell spans three planes, so that there are $\frac{21}{3} = 7$ allowed values of q_z.) In Fig. 7(e), all of the results of Figs. 7(b)–7(d) are superimposed to show the complete spectrum of vibrational frequencies for values of (q_x, q_y) lying along a line extending from the origin to the edge of the slab-shaped BZ. This line corresponds to the line $\bar{\Gamma}\bar{M}$ in Fig. 1. Finally, in Figs. 7(f) and 7(g), we show the results obtained by following a similar procedure for the lines $\bar{M}\bar{K}$ and $\bar{K}\bar{\Gamma}$.

The curves in Figs. 7(e)–7(g) correspond exactly to those in Fig. 8. The only difference is that the former results are for a 21-layer slab with periodic boundary conditions in the z direction and the latter are for a 21-layer slab with two free surfaces. The differences between these two sets of curves—in particular, the presence of surface modes in Fig. 8—are due to the "perturbation" which results when one "severs" the periodic boundary conditions in the z direction to create two free surfaces.[8]

It should be emphasized, however, that the results shown in Figs. 7 and 8 were obtained in completely independent calculations. All of the results of this paper (and the others in this series) are based on direct calculations for slab-shaped crystals with two free surfaces, without recourse to any method in which the surfaces are regarded as a perturbation. The results of Fig. 7 serve as a check on those of Fig. 8. We have carried out similar calculations for the (100) and (110) surfaces, in order to check the bulk bands obtained in calculations for the slabs with surfaces against those obtained by the procedure described above. In all cases there is agreement.

III. SURFACE MODE SPECTRA

A. (111) Surface

In Fig. 8, the ω-vs-$\bar{q}$ relations are shown for a 21-layer crystal with (111) surfaces. The modes labeled S_1, S_2, S_3, S_4, and S_5 all lie outside the bulk bands and must therefore be surface modes.[9] That these modes are indeed localized at the surface is shown by the fact that their calculated eigenvectors are large near the surface and show a rapid decrease with increasing distance from the surface. In Fig. 9, the squared amplitude

$$|\vec{\xi}(m)|^2 = |\xi_x(m)|^2 + |\xi_y(m)|^2 + |\xi_z(m)|^2 \qquad (3.1)$$

for S_1, S_2, S_3, and S_4 is plotted as a function of the layer index m, with $m = 1$ for the surface layer. (We take $l_3 = 0$ at the center of the crystal, so for a 21-layer crystal $m = 1$ corresponds to $l_3 = 10$.) Both the frequencies ω and the eigenvectors $\xi_\alpha(l_3)$ are obtained by solving Eq. (2.2) numerically. We recall that the displacement amplitude $|u_\alpha(l_3)|$ in Eq. (2.1) is proportional to $|\xi_\alpha(l_3)|$ for a monatomic crystal, according to Eq. (2.15) of I, so $|\vec{\xi}(m)|^2$ is a measure of the amplitude of vibration in the

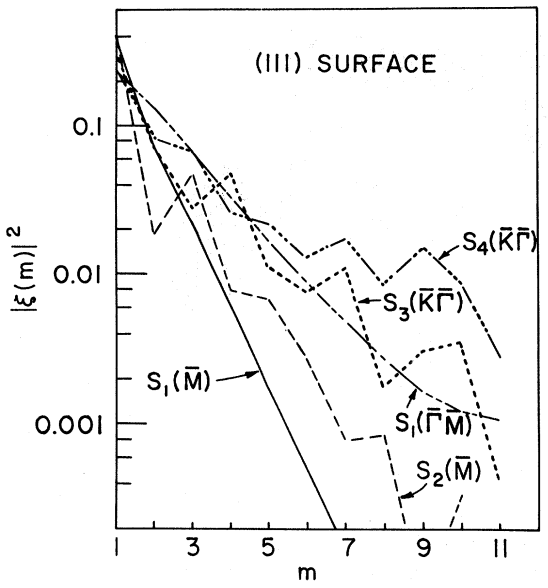

FIG. 9. Squared amplitude $|\vec{\xi}(m)|^2$ vs layer number m for the surface modes shown in Fig. 8. Here $m=1$ for a surface layer and $m=11$ for the center layer. The vertical scale is logarithmic. The mode $S_1(\bar{\Gamma}\bar{M})$ is that mode on the S_1 branch which lies halfway between $\bar{\Gamma}$ and $\bar{M}$ in Fig. 8. The modes $S_3(\bar{K}\bar{\Gamma})$ and $S_4(\bar{K}\bar{\Gamma})$ lie on the S_3 and S_4 branches, respectively, just to the right of $\bar{K}$ in Fig. 8. $S_1(\bar{M})$ and $S_2(\bar{M})$ lie on the S_1 and S_2 branches, respectively, at the point $\bar{M}$.

mth layer when the crystal is vibrating in a particular mode.

Notice that the vertical scale in Fig. 9 is logarithmic and that all of the modes S_i decrease by more than an order of magnitude between the surface and the center of the crystal. The mode S_1 decreases rather smoothly with distance from the surface, both at the point $\bar{M}$ and at a point half-way between $\bar{\Gamma}$ and $\bar{M}$. The decrease is, in fact, approximately exponential. As one expects, the rate of decrease is larger for the larger value of $\bar{q}$ (i.e., the point $\bar{M}$); as the origin is approached, the penetration depth increases.

The surface-mode branch S_1 is typical of the "generalized Rayleigh waves" found in continuum theory,[10,11] in that it lies beneath the bulk bands, persists into the long-wavelength limit, and shows an approximately exponential decay in amplitude with increasing distance from the surface. None of these statements, however, is true of S_2, S_3, and S_4. These modes lie in gaps between the bulk bands, they are absorbed into the bulk bands and cease to be surface modes for small values of $\bar{q}$, and their amplitudes show, in Fig. 9, a rather complicated dependence on the distance from the surface: $|\vec{\xi}|^2$ does not decrease monotonically, or even regularly, and it certainly does not decrease exponentially.

"Gap" modes like S_2, S_3, and S_4 appear to be a very commonplace occurrence. We have also found them in calculations for the (100) and (110) surfaces (see below). They have subsequently been found in a point-ion model of NaCl.[12]

Along the line $\bar{\Gamma}\bar{K}$ there is a mixed (or "pseudo-surface") mode MS_3 which represents, in effect, an extension of S_3 into the bulk bands. This mode is visible in Fig. 8 as a disturbance in the bulk bands, above the bottom of these bands and just beneath the next envelope of bulk modes.

All of these modes—S_1, S_2, S_3, S_4, and MS_3—are localized primarily in the surface layer, as can be seen in Fig. 9. The polarizations in the surface layer are as follows: S_1 is primarily a "shear-vertical" (SV) mode; i.e., it is primarily associated with vibrations normal to the surface. S_3 and MS_3 are primarily "shear-horizontal" (SH) modes; i.e., they are primarily associated with vibrations in the direction transverse to $\bar{q}$ and parallel to the surface. S_2 and S_4 are primarily longitudinal or "P" modes; i.e., they are primarily associated with vibrations in the direction parallel to $\bar{q}$.[13]

The surface mode S_5 lies under all of the bulk bands, rather than within a gap in these bands, but like the "gap" modes it also does not persist into the long-wavelength limit. In fact, it exists as a surface mode only in a narrow region near $\bar{K}$. At a very small distance from $\bar{K}$, along the line $\bar{\Gamma}\bar{K}$, S_5 enters the bulk bands and ceases to be a surface mode. Unlike the other surface modes for the (111) surface, S_5 is localized primarily in the *second*-layer beneath the surface, and in this layer it has the same polarization that S_1 has in the surface layer—i.e., mainly SV.

B. (100) Surface

The surface-mode spectrum for the (100) surface is considerably more complex than that for the (111) surface, as can be seen in Fig. 10. There are also a number of interesting features not seen in the results for the (111) surface:

First, there are two surface-mode branches located within the bulk bands—namely S_3, along the line $\bar{\Gamma}\bar{M}$, and S_4, along the line $\bar{\Gamma}\bar{X}$. As pointed out in I, along symmetry lines that are associated with reflection planes of the crystal, such as $\bar{\Gamma}\bar{M}$ and $\bar{\Gamma}\bar{X}$, the modes "partition" into two classes, with the modes of one class polarized strictly within the sagittal plane and those of the other class polarized strictly perpendicular to this plane. It is possible for a surface mode belonging to one class to lie in the bulk bands associated with the other class. In fact, if a mode lies outside the bulk bands for its class, then it must be a surface mode. Inspection of the eigenvectors shows that both S_3 (along $\bar{\Gamma}\bar{M}$)

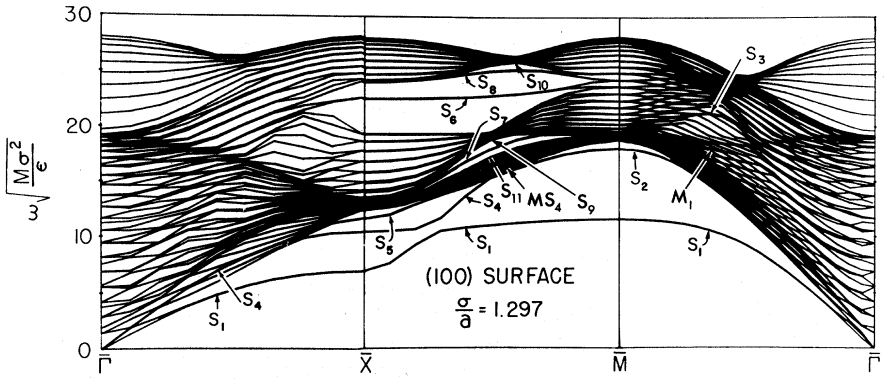

FIG. 10. ω vs $\bar{q}$ for a 21-layer slab with (100) surfaces. Besides the indicated surface modes S_1, S_2,. . ., S_{11}, there appear to be two other surface modes at $\bar{M}$ (above S_2), at least five others at $\bar{X}$ (above S_5), one more above S_{10}, and possibly several more above S_9. There thus appear to be at least 19 distinct surface-mode branches for the (100) surface, plus several associated series of mixed modes.

and S_4 (along $\bar{\Gamma}\bar{X}$) are polarized strictly within the sagittal plane and that the bulk modes surrounding them are polarized strictly normal to the sagittal plane. S_3 and S_4 must therefore be surface modes. That they indeed are is shown by the graphs of their squared amplitudes $|\vec{\xi}(m)|^2$ versus the layer number m. For both modes $|\vec{\xi}|^2$ falls by more than two orders of magnitude between the surface and the center of the crystal.

Although the surface-mode branch S_1 persists throughout the region between the lines $\bar{\Gamma}\bar{X}$ and $\bar{\Gamma}\bar{M}$, it undergoes a drastic change of polarization between these lines: Along $\bar{\Gamma}\bar{X}$, it is strictly SH (polarized normal to the sagittal plane). Along $\bar{\Gamma}\bar{M}$, it is polarized strictly within the sagittal plane and is predominantly SV (polarized normal to the surface). On the other hand, S_4 is predominantly

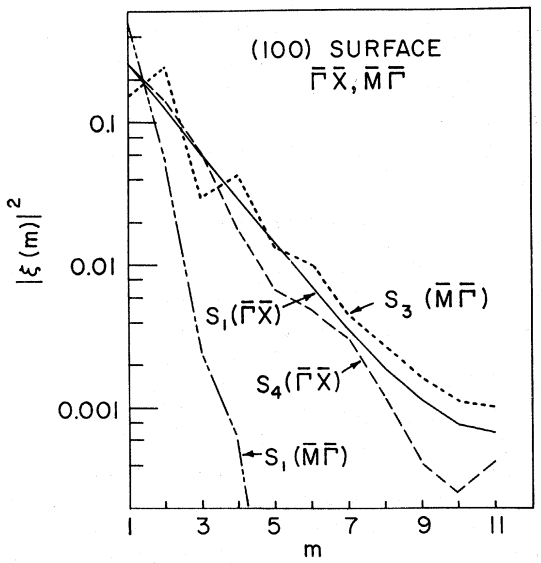

FIG. 11. Graph of $|\vec{\xi}(m)|^2$ vs m for surface modes S_1 and S_4 at the point along $\bar{\Gamma}\bar{X}$ indicated by the arrows in Fig. 10, and for S_1 and S_3 at the point along $\bar{M}\bar{\Gamma}$ indicated by the arrows.

SV along ΓX and is predominantly SH just before it enters the bulk bands between $\bar{X}$ and $\bar{M}$. What happens in the region between $\bar{\Gamma}\bar{X}$ and $\bar{\Gamma}\bar{M}$ is the following: S_1 and S_4 approach each other closely (just to the right of $\bar{X}$ in Fig. 10), but do not quite cross.[14] In the region where they nearly cross, there is a sudden interchange of character: Going from left to right, S_1 changes from SH to SV, and S_4 from SV to SH. This behavior—the mutual avoidance of two branches with an interchange of character—has analogies in other physical situations, such as the hybridization of "crossing" bands in electronic band theory.[15]

It should be mentioned that S_4 is distinct from S_2, which is of some interest in its own right. Both S_2 and S_5 are localized primarily in the second layer beneath the surface. As can be seen in Figs. 11 and 12, the same is true of S_3 and S_8. Also, S_7 is localized primarily in the *third* layer beneath the surface. Although they are not graphed, S_{11} is mainly localized in the second layer, S_{10} in the third layer, and S_9 in the fourth layer. We thus again have the result that it is possible for a mode localized near the surface to have its maximum amplitude in some layer beneath the surface layer. At the point $\bar{X}$, S_1 and S_5 are concentrated almost entirely in the first and second layers, respectively, and at the point $\bar{M}$ the same is true of S_1 and S_2; i.e., at these points we have "single-layer" modes in which the first or second layer vibrates almost independently of all the others. Moreover, there are a number of other modes (at least five) at the point $\bar{X}$, just above S_5, which are strongly localized in the third, fourth, etc., layers. There are two other modes at the point $\bar{M}$, just above S_2, which are strongly localized in the third and fourth layers. All of these modes appear to lie very slightly under the bulk bands and to be completely localized near the surface.

An analogous situation exists about midway between $\bar{X}$ and $\bar{M}$, at the "bottleneck" in the upper bulk band caused by the twisting of this band between $\bar{X}$ and $\bar{M}$. Above S_{10} there is a mode which is pri-

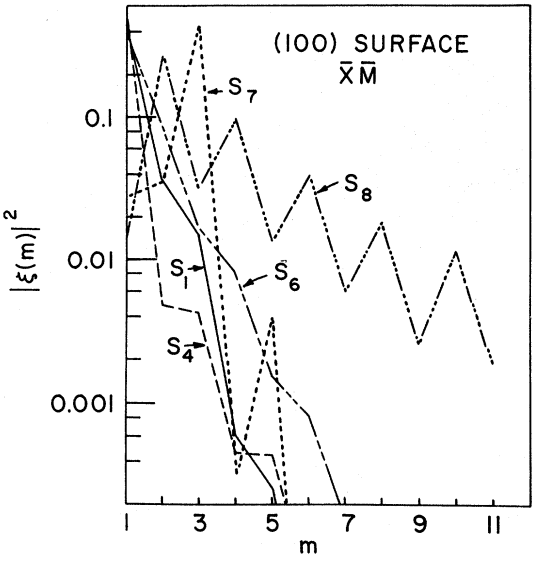

FIG. 12. Graph of $|\vec{\xi}(m)|^2$ for surface modes S_1, S_4, S_6, S_7, and S_8 at the point along $\bar{X}\bar{M}$ indicated by the arrows in Fig. 10.

marily localized in the fourth layer, and which appears to lie very slightly beneath the bulk bands and to be completely localized near the surface. Furthermore, there is another such situation at the bottleneck in the middle bulk band between $\bar{X}$ and $\bar{M}$. Above S_9 there are several modes which are primarily associated with the fifth, sixth, etc., layers; some of these modes may be completely localized near the surface.

We thus have the result that at each of the four bottlenecks in Fig. 10—for the lowest bulk band at $\bar{X}$ and $\bar{M}$, and for the upper and middle "bands" between $\bar{X}$ and $\bar{M}$—there is a series of "single-layer" modes associated with the first, second, third, etc., layers. The series at $\bar{X}$ includes S_1, S_5, etc., and every mode has SH polarization. The series at $\bar{M}$ includes S_1, S_2, etc.; every mode is polarized within the sagittal plane and is primarily SV. At the bottleneck in the upper band of bulk modes, the series includes S_6, S_8, S_{10}, etc. Each of these modes is polarized strictly parallel to the plane of the surface in the layer where its amplitude is largest; specifically, $\xi_x = \xi_y$ and $\xi_z = 0$ in this layer.[16,17] At the "bottleneck" in the middle band, the series includes the mixed mode MS_4 (which represents an extension of S_4 into the lowest bulk band), S_{11}, S_7, S_9, etc.; MS_4 is associated with the first layer, S_{11} with the second, S_7 with the third, and S_9 with the fourth. For each mode in this series, $\xi_x = -\xi_y$ in the layer where its amplitude is largest.[16]

It can be seen in Figs. 11 and 12 that the amplitudes of the surface modes depend in a rather complicated way upon the distance from the surface, just as in the case of the (111) surface. As one expects, S_1 and S_4 show a larger attenuation for larger values of $\bar{q}$ (compare the results of Fig. 11 with those of Fig. 12). For small $\bar{q}$, S_1 shows an approximately exponential decrease with distance from the surface; for large $\bar{q}$ this is no longer true.

The attenuation graphs for points on the edge of the BZ, given in Fig. 12, show the following behavior for every mode: Except for the surface layer ($m=1$), the values of $|\vec{\xi}(m)|^2$ for odd m lie approximately along one straight line; the values for even m lie approximately along another straight line; and the two lines are parallel. The results for S_1, S_4, and S_6, which are largest in amplitude at the surface, fall off monotonically in a "staircase" pattern. The results for S_7 and S_8, which are largest in amplitude in the second or third layer, fall off nonmonotonically in a "mountain range" pattern. These features appear to result from the symmetry associated with a point on the edge of the BZ in the case of the (100) surface.[16]

In addition to the surface-mode branches described above, there is a mixed mode labeled M_1 in Fig. 10. This mode has its maximum amplitude in the first layer, where it is polarized primarily in the x direction. It thus has approximately the same character as S_3, which reaches maximum amplitude in the second layer. It should be mentioned, however, that S_3 changes its character somewhat as a function of $\bar{q}$: At the point indicated by the arrow in Fig. 10, S_3 has some x polarization but more z polarization in the second layer; at this point, it also has appreciable amplitude in the first layer, where it is polarized primarily in the x direction. To the right of this point in Fig. 10 (nearer $\bar{\Gamma}$), S_3 becomes more strongly localized in the second layer and becomes strongly polarized in the x direction within this layer; i.e., it acquires the same character in the second layer as M_1 has in the first layer.

C. (110) Surface

The surface-mode spectrum for the (110) surface, shown in Fig. 13, is about as complex as that for the (100) surface and has many of the same features. In fact, there is some kinship between the results for $\bar{\Gamma}\bar{X}$ in Fig. 10 and the results for $\bar{\Gamma}\bar{X}$ and $\bar{\Gamma}\bar{Y}$ in Fig. 13, and between the S_6 gap in Fig. 10 and the S_7 and S_5 gaps in Fig. 13: If the longer edge of the two-dimensional unit cell for the (110) surface were continuously shortened until it equaled the shorter edge, then the (110) surface would change continuously into the (100) surface; the points $\bar{X}$ and $\bar{Y}$ would become equivalent to the point $\bar{X}$ for the (100) surface; and the point $\bar{S}$ would become equivalent to the point $\bar{M}$. Consequently, the results for $\bar{S}\bar{Y}\bar{\Gamma}$ in Fig. 13 would become the mirror

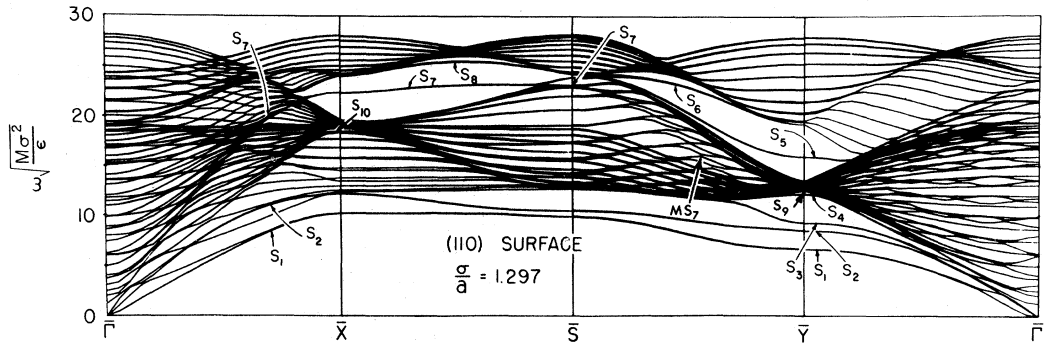

FIG. 13. ω vs $\bar{q}$ for a 21-layer slab with (110) surfaces. In addition to the 10 distinct surface-mode branches, there is a mixed mode MS_7 which can be seen as a disturbance in the bulk bands along $\bar{S}\,\bar{Y}$ below $\bar{S}_5$.

image of those for $\bar{\Gamma}\bar{X}\bar{S}$, which would become the same as those for $\bar{\Gamma}\bar{X}\bar{M}$ in Fig. 10. The evident similarities between $\bar{\Gamma}\bar{X}\bar{S}$ in Fig. 13 and $\bar{\Gamma}\bar{X}\bar{M}$ in Fig. 10 are thus not difficult to understand.

It should also be mentioned that in the dispersion curves for the line $\bar{\Gamma}\bar{S}$ for the (110) surface (not shown here) one can observe a feature corresponding to the "quasigap" in which S_3 falls along $\bar{\Gamma}\bar{M}$ for the (100) surface in Fig. 10. This feature persists to the point $\bar{S}$, and, in fact, is responsible for the existence of S_7 as a surface mode at this point (see below).

In Fig. 13, there are five cases of surface modes lying within the bulk bands—namely, S_2 along $\bar{\Gamma}\bar{X}$,[18] S_7 along $\bar{\Gamma}\bar{X}$, S_7 at $\bar{S}$, S_9 along $\bar{\Gamma}\bar{Y}$, and S_{10} along $\bar{\Gamma}\bar{X}$. Four of these cases (all but S_7 at $\bar{S}$) are explained in the same way as S_3 and S_4 for the (100) surface, since $\bar{\Gamma}\bar{X}$ and $\bar{\Gamma}\bar{Y}$ are associated with reflection planes and there is consequently a "partitioning" of the modes into two classes, as discussed in I. The line $\bar{\Gamma}\bar{S}$ is not associated with a reflection plane; using symmetry arguments, however, one can show that there is still a "partitioning" of the modes into two mutually orthogonal classes at the point $\bar{S}$, so that it is possible for a surface mode of one class to exist in the bulk bands for the other class at this point. An examination of the calculated eigenvectors at $\bar{S}$ shows that S_7 and the bulk modes surrounding it belong to different classes, so S_7 must necessarily be a surface mode.[19] This result is confirmed by the attenuation graph in Fig. 14.[20]

The dependence of amplitude upon distance from the surface is again rather complicated, as shown in Figs. 14, 15, and 22(a). There are also modes which are primarily localized in some layer beneath the surface: S_9 in Fig. 15 and S_8 in Fig. 22(a) have their maximum amplitude in the second layer; S_4 in Fig. 15 and S_6 in Fig. 22(a) have their maximum amplitude in the third layer. Although S_{10} is not graphed, it is strongly localized in the second layer.

There are two cases in Fig. 13 of the hybridization of two surface-mode branches: Between $\bar{X}$ and $\bar{S}$, S_1 and S_2 approach each other but do not cross. At $\bar{X}$, S_1 is polarized mainly in the z direction (SV) and S_2 is polarized entirely in the y direction (SH).[17] At $\bar{S}$, S_1 is polarized mainly in the y direction, and S_2 entirely in the z direction. The interchange of character occurs in the region of closest approach near $\bar{S}$.

Near the point $\bar{Y}$, along $\bar{S}\,\bar{Y}$, S_3 descends out of the lowest bulk band. At the point where it first appears, S_3 is polarized primarily in the x direction. (This is the same polarization as that of MS_7. As one might suspect from looking at Fig. 13, S_3 represents an extension of MS_7 into the region be-

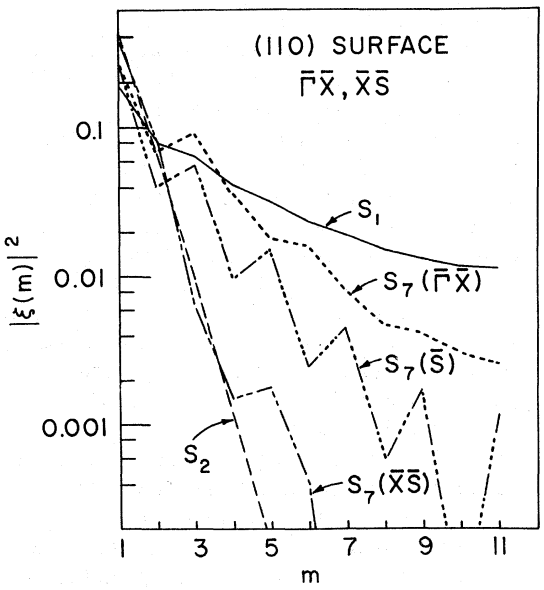

FIG. 14. Graph of $|\vec{\xi}(m)|^2$ for surface modes shown in Fig. 13. S_1, S_2, and S_7 $(\bar{\Gamma}\bar{X})$ are plotted at the point along $\bar{\Gamma}\bar{X}$ indicated by the arrows in Fig. 13. $S_7(\bar{X}\bar{S})$ and $S_7(\bar{S})$ are plotted at the indicated points along $\bar{X}\,\bar{S}$.

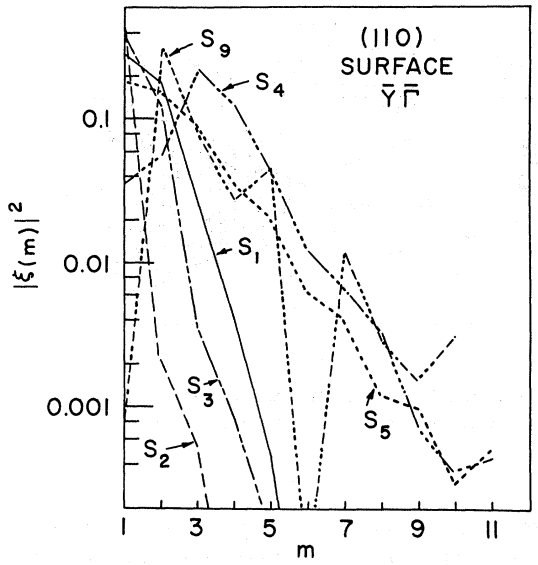

FIG. 15. Graph of $|\vec{\xi}(m)|^2$ for surface modes S_1, S_2, S_3, S_4, S_5, and S_9 at a point along $\bar{Y}\bar{\Gamma}$ just to the right of $\bar{Y}$ in Fig. 13.

low the bulk bands.) After its emergence, S_3 approaches S_2 and they exchange character: At $\bar{Y}$, S_2 is polarized entirely in the x direction (SH) and S_3 primarily in the z direction (SV). At this point, S_1 is still polarized mainly in the y direction (longitudinal).

It may seem strange that the lowest-frequency surface mode along $\bar{\Gamma}\bar{Y}$, S_1, is primarily longitudinal, since one ordinarily associates high frequencies with longitudinal waves. However, if $\bar{q}$ lies on the line $\bar{\Gamma}\bar{Y}$ then a longitudinal polarization corresponds to vibrations in the ⟨100⟩ direction. Since there are no nearest neighbors in the ⟨100⟩ direction, particles at the surface [for a (110) orientation] can vibrate with considerable freedom in that direction. It is therefore not surprising that the lowest-frequency surface mode should be associated with vibrations in the ⟨100⟩ direction.

At $\bar{Y}$, the modes S_1, S_2, and S_3 are all primarily localized in the surface layer, but S_2 is much more strongly localized in this layer than are S_1 and S_3. This fact presumably accounts for the result that S_2, with in-plane (SH) polarization, has a lower frequency than S_3, which is mainly SV.

Along $\bar{\Gamma}\bar{X}$, the modes S_2 and S_{10} are related, in that both have strictly SH polarization and they have their maximum amplitudes in the first and second layers, respectively. Just above S_{10} there is what appears to be a mixed mode with SH polarization which has its maximum amplitude in the third layer. Along $\bar{X}\bar{S}$, S_7 and S_8 are similarly related: S_7 is strongly localized in the first layer, and S_8 in the second layer; each mode is polarized strictly in the x direction in the layer where it has its maximum amplitude. There are also two mixed modes above S_8 at the bottom of the uppermost bulk band where the bottleneck occurs between $\bar{X}$ and $\bar{S}$. These modes have their maximum amplitudes in the third and fourth layers, respectively, and each is polarized in the x direction in the layer of maximum amplitude.

About midway between $\bar{S}$ and $\bar{Y}$, S_5 has its maximum amplitude in the second layer, where it is polarized principally in the x direction. It thus has the same character in this region as MS_7, which is polarized mainly in the x direction in the first layer, where it has its maximum amplitude. The mode S_6 reaches maximum amplitude in the second layer and is polarized strictly in the y direction there. There is a mixed mode above S_6, at the bottom of the bottleneck in the uppermost bulk band between $\bar{S}$ and $\bar{Y}$, which has its maximum amplitude in the third layer and is polarized in the y direction within that layer.

Between the midpoint of $\bar{S}\bar{Y}$ and the point $\bar{Y}$, S_5 undergoes a change of character, and at $\bar{Y}$ it has roughly the same character as S_1 (maximum amplitude and longitudinal polarization in first layer, considerable amplitude and SV polarization in second layer). Its frequency is much higher than that of S_1, however, because it has a smaller amplitude in the surface layer. The surface mode S_9 assumes the character lost by S_5: S_9 reaches maximum amplitude in the second layer and has SH polarization. (To the left of $\bar{Y}$, S_9 rises up into the bulk bands and becomes unrecognizably mixed with the bulk modes.) It is apparent that S_2 and S_9 at $\bar{Y}$ are related modes, since both are SH. There is also an evident relation between S_3 and S_4 at this point: Each of these modes has SV polarization in its layer of maximum amplitude—the first layer for S_3 and the third layer for S_4.

D. Comparison with Continuum Calculations

It should be mentioned that many of the qualitative features of our results for small $\bar{q}$ (large wavelengths) can also be observed in the results of treatments based on the continuum approximation, which is valid in the long-wavelength limit.[11] The most extensive work in this field is that of Lim and Farnell,[21,22] and a review of the field has been written by Farnell.[10] We mention, for example, that the results for the (001) surface of Ge, the (110) surface of KCl, and the (111) surface of Si, shown in Figs. 1–3 of Ref. 22, are similar to the long-wavelength results in Figs. 10, 13, and 8, respectively, of the present paper. As a rough rule, one expects the long-wavelength behavior to be qualitatively similar for materials with cubic symmetry. However, in some cases the values of the elastic constants can also be important: The

anisotropy ratio η is defined in terms of the elastic constants c_{ij} by

$$\eta = 2c_{44}/(c_{11} - c_{12}) , \tag{3.2}$$

and for our model ("Lennard-Jonesian") $\eta = 2.66$.[11] For $\eta > 1$, as in our model, the lower edge of one of the two "transverse bulk bands" along $\bar{\Gamma}\bar{X}$ in Fig. 10 will lie higher than the lower edge of the other. The surface-mode branch S_1 "peels off" from the lower band, and the branch S_4 peels off from the higher band, so S_1 lies below S_4. However, for $\eta < 1$ the lower edges of the bulk bands will switch positions—i.e., the lower band for $\eta > 1$ becomes the higher for $\eta < 1$—so that S_4 should lie below S_1 along $\bar{\Gamma}\bar{X}$, in the long-wavelength limit, for the case $\eta < 1$. Therefore, for this case, the SH surface wave should lie *above* the (primarily) SV surface wave in the long-wavelength limit, whereas it lies below in the results for our model shown in Fig. 10. As a result, the hybridization of S_1 and S_4 shown along $\bar{X}\bar{M}$ in Fig. 10 should not occur in the long-wavelength limit for $\eta < 1$, since the SH wave always lies above the SV wave and the two will not attempt to cross. This expectation is confirmed by the results in Fig. 8 of Ref. 10.[23]

IV. BEHAVIOR OF SURFACE MODES THROUGHOUT INTERIOR OF BRILLOUIN ZONE

So far we have discussed the behavior of the surface modes only along the symmetry lines enclosing the irreducible element (IE) of the two-dimensional BZ's (heavy lines in Fig. 1). It is also of interest, however, to see what happens within the IE. We have therefore carried out calculations which "sweep out" the interior of the IE for all three surfaces.

One question that arises from an examination of Fig. 8 is whether S_2 and S_4 for the (111) surface are actually distinct modes or are connected within the IE. Our calculations show that they are in fact distinct: The gap enclosing S_2 closes up slightly to the left to $\bar{\Gamma}\bar{K}$ even within the interior of the IE. (It obviously does so along the BZ edge.) The gap enclosing S_4 then opens up, very close to $\bar{\Gamma}\bar{K}$. The two gaps are thus distinct, and S_2 and S_4 are not connected within the IE.

In Fig. 16, we show the dispersion curves for the (100) surface along several rays from the origin ($\bar{\Gamma}$) to a point on the edge of the BZ ($\bar{Y}$). The indicated angle (e.g., 4.5°) is the angle between the ray and the line $\bar{\Gamma}\bar{M}$. It is interesting that S_8, in Fig. 16(a), and S_4, in Fig. 16(c), make their appearance within the IE before they are present at the edge of the zone (i.e., for smaller angles), because the bulk modes exhibit greater dispersion than these surface modes. One can, however, observe a mixed mode corresponding to S_4 at the edge of the zone, where S_4 has entered the lowest band, in Fig. 16(c).

In the case of the (110) surface, an examination of Fig. 13 raises the question as to whether S_8 is distinct from S_5 and S_6. Our calculations indicate that S_8 is in fact a distinct branch, but that it is closely related to S_5: The gap enclosing S_8 closes up slightly to the right of $\bar{\Gamma}\bar{S}$, even within the IE, before the gap enclosing S_5 and S_6 opens up. As its gap closes, S_8 enters the bulk bands and one can

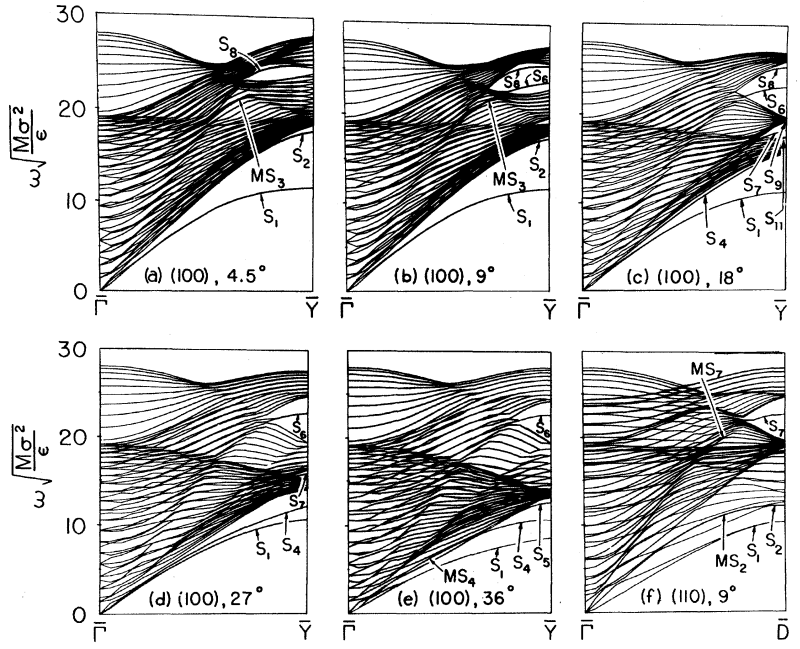

FIG. 16. Dispersion curves (ω vs $\bar{q}$) for rays extending from the origin $\bar{\Gamma}$ to a general point $\bar{Y}$ or $\bar{D}$ on the edge of the BZ (see Fig. 1 for the definition of $\bar{Y}$ and $\bar{D}$). For the (100) surface, the angle between the ray and the line $\bar{\Gamma}\bar{M}$ is indicated (e.g., 27°). For the (110) surface, the angle between the ray and the line $\bar{\Gamma}\bar{X}$ is indicated (9°).

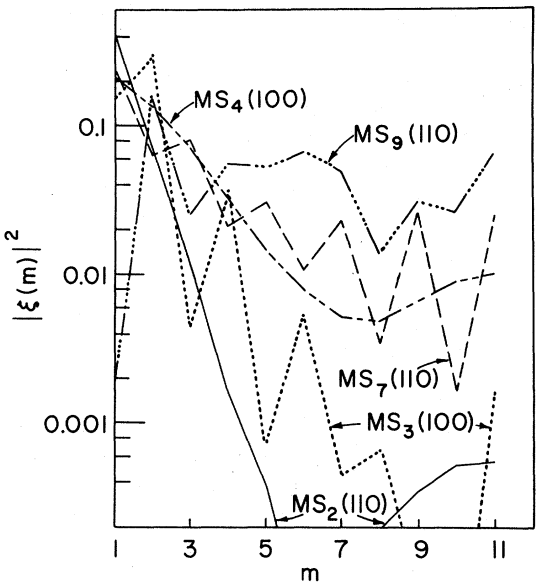

FIG. 17. Graph of squared amplitude vs distance from surface for mixed modes MS_3 and MS_4 for (100) surface, shown in Figs. 16(a) and 16(e); MS_2 and MS_7 for (110) surface, shown in Fig. 16(f); and MS_9 for (110) surface, at a point on a ray 4.5° off the line $\bar{\Gamma}\bar{Y}$ (not shown in Fig. 16). For MS_3, MS_4, MS_2, and MS_7 the modes are graphed at the positions indicated by the arrows in Fig. 16.

find a mixed mode MS_8 which in effect represents an extension of S_8. When the second gap opens, it contains S_5, which is in effect an extension of MS_8. The modes S_8, MS_8, and S_5 (near $\bar{S}$) all have the same character, in that all reach maximum amplitude in the second layer and are primarily polarized in the x direction within this layer.

The surface modes S_3 and S_4 for the (100) surface, shown in Fig. 10, lie within the bulk bands. The same is true of S_2, S_7, and S_{10} in Fig. 13, as well as S_9 to the right of $\bar{Y}$. As discussed in Refs. 1 and 3, surface modes within the bulk continua are possible only along symmetry lines where there is a "partitioning" of the modes into mutually orthogonal classes. The modes of one class are "invisible" to those of the other class along the symmetry line. For points slightly removed from the symmetry line, however, the modes are again visible to one another, and any surfacelike mode lying in the bulk bands will mix with the bulk modes. Consequently, S_3 and S_4 for the (100) surface must degenerate into mixed modes MS_3 and MS_4 for points slightly off $\bar{\Gamma}\bar{M}$ and $\bar{\Gamma}\bar{X}$, respectively. In Figs. 16(a) and 16(e), MS_3 and MS_4 are labeled, and graphs of their square amplitudes versus distance from the surface are shown in Fig. 17. Similarly, we show MS_2 and MS_7 for the (110) surface at points 9° off the line $\bar{\Gamma}\bar{X}$ in Fig. 16(f), and their squared amplitudes are graphed in Fig. 17. A plot of the squared amplitude is also given in Fig. 17 for MS_9 at a point 4.5° off the line $\bar{\Gamma}\bar{Y}$ for the (110) surface. It is fairly evident that all these modes are in fact mixed modes, as they have to be.

V. SIMPLE SCHEME FOR INTERPRETING SURFACE-MODE SPECTRA

Despite the considerable complexity of the surface-mode spectra discussed above, all the surface modes and mixed modes can be understood in the context of a simple phenomenological scheme. This scheme does not allow one to determine the surface modes without a calculation, but it does help in understanding how they arise.

We begin with the bulk bands for a crystal without surfaces, such as those indicated in Figs. 7(e)–7(g). For a monatomic crystal there should ordinarily be three such bands (which may overlap), corresponding roughly to two groups of transverse modes and one of longitudinal modes. We then introduce the perturbation represented by the surface, which actually consists of two parts—a "first-order" perturbation due simply to the truncation of the crystal and a "second-order" perturbation due to changes in the force constants near the surface. The second part should not be important in monatomic crystals at large wavelengths, where the surface modes penetrate deeply, but it is important at small wavelengths, as will be discussed in Sec. VI.

The strength of the total perturbation depends on the point in the BZ—i.e., the value of the two-dimensional wave vector $\bar{q}$. If the perturbation is strong enough for a given value of $\bar{q}$, it will peel one or more surfacelike modes off a given bulk band. Ordinarily the perturbation should correspond to a softening of the vibrations, since the truncation of the crystal allows the surface atoms to vibrate more freely, and one expects the surface atoms to relax outward (as they do in our model), producing a decrease in the surface force constants. For such a softening perturbation, the surface modes should be peeled off the bottom of the bulk band. If for some reason (e.g., a change in the interaction between the particles near the surface), the total perturbation leads to a stiffening of the lattice vibrations, then the surface modes should be peeled off the top of the bulk band. Such high-frequency surface modes were produced in the calculations of Musser and Rieder[24] when the surface force constants were stiffened, but it does not seem likely that they will occur naturally in monatomic crystals, and they do not occur in the present results, of course.

Ordinarily, the total perturbation due to the surface should first peel off (from a given bulk band) a mode primarily localized in the first layer. If strong enough, it should then peel off a mode pri-

marily localized in the second layer, and so on. The nth-layer mode in this series has the same character in the nth layer as the first-layer mode has in the first layer. Sometimes the perturbation will not completely succeed in peeling off the mode, in which case the mode remains within the bulk band as a mixed mode.

When a mode is peeled off, one of four things will happen: (a) It may fall under all of the bulk bands, in which case it will necessarily be a surface mode. (b) It may fall into a gap between two bulk bands, in which case it again will necessarily be a surface mode. (c) Along a symmetry line associated with a reflection plane, it may fall into a region occupied only by bulk modes to which it is automatically orthogonal, as discussed in I. In this case, once more, it will necessarily be a surface mode. (d) It may fall into a region occupied by bulk modes to which it is not automatically orthogonal. In this case it will not be able to survive as a pure surface mode and will be a mixed mode instead. The reason for the mixing can be understood by the following rough argument: Let $\vec{\xi}_s$ be the $3N_3$-dimensional eigenvector that the surfacelike mode would have if there were no bulk modes in the region where it falls. If this mode is then degenerate with a bulk mode $\vec{\xi}_b$, it must be made orthogonal to $\vec{\xi}_b$ in order to meet the orthonormality requirement that is imposed on the normal modes. (It is "vanishingly probable" that $\vec{\xi}_s$ and $\vec{\xi}_b$ will be orthogonal unless they are automatically orthogonal as discussed just above.) The new orthogonal eigenvector is (before normalization) $\vec{\xi}_s - (\vec{\xi}_s \cdot \vec{\xi}_b)\vec{\xi}_b$. This eigenvector contains a bulk part and is therefore not entirely localized at the surface.

Occasionally two surface-mode branches will attempt to cross each other. In such a case there will be hybridization, with the hybrid branches exhibiting a mutual repulsion and interchange of character. The only case where two surface-mode branches could, in fact, cross is along a symmetry line associated with a reflection plane, with the two modes belonging to mutually orthogonal classes and therefore invisible to one another. Such a situation does not occur in the present results but has been found in calculations for NaCl[23] and for an adsorbed layer [see Ref. 1(b)]. Similarly, a surface-mode branch which enters a bulk band will be repelled by the band and tend to bend away from it. The only exception is along a symmetry line when the band is invisible to the surface mode because its modes and the surface mode are automatically orthogonal.

The results of Figs. 8, 10, and 13 can be interpreted as follows according to the above scheme: For the (111) surface, S_2 is peeled off the "longitudinal band" of bulk modes along $\overline{MK}$, S_4 is peeled off the uppermost band along $\overline{\Gamma K}$, S_3 and its extension MS_3 are peeled off the upper "transverse band," and S_1 is peeled off the lower "transverse band." The perturbation is just strong enough to peel off a mode near the edge of the BZ, S_5, which is the second-layer analog of S_1.

For the (100) surface, the first-layer mode S_1 and the second-layer mode S_2, plus third- and fourth-layer modes, are peeled off the "transverse bands" near the point $\overline{M}$. Near $\overline{X}$, the first-layer mode S_1, the second-layer mode S_5, and a number of nth-layer modes are peeled off the lower "transverse band." The first-layer modes S_4 and MS_4, the second-layer mode S_{11}, the third-layer mode S_7, the fourth-layer mode S_9, and a number of nth-layer modes are peeled off the upper "transverse band." The first-layer mode S_6, the second-layer mode S_8, and the third-layer mode S_{10} are peeled off the "longitudinal band" along $\overline{XM}$; along $\overline{\Gamma M}$, the first-layer mode M_1 and the second-layer mode S_3 are peeled off this band.

For the (110) surface, S_1 is peeled off from the lower "transverse band," S_2 and S_{10} from the upper "transverse band," and S_7 and S_8 from the "longitudinal band" on the left-hand side of Fig. 13. On the right-hand side of Fig. 13, S_5 and S_6 are peeled off the "longitudinal band." Near $\overline{Y}$, S_5 is a first-layer mode with the same character as the second-layer mode S_6. As S_5 approaches the lower bulk bands from the right along $\overline{S}\,\overline{Y}$, it in effect hybridizes with the modes in the upper part of this band and acquires a different character—in fact, the character of a second-layer analog of MS_7. The first-layer mode MS_7 is peeled off the top of the "transverse bands"; as it approaches $\overline{Y}$ along $\overline{S}\,\overline{Y}$, it descends out of the bulk bands to become the surface mode S_3, which then hybridizes with S_2. At $\overline{Y}$, there are two series of surface modes which have peeled off from the "transverse bands": The first-layer mode S_2 and the second-layer mode S_9 belong to one series, with both having SH polarization. The first-layer mode S_3 and the third-layer mode S_4 belong to the second series, with both being primarily SV in the layer of maximum amplitude. It appears that S_1 should also be fitted into this series as the missing second-layer mode. A serious difficulty with this interpretation, of course, is the fact that S_1 has appreciable amplitude in both the first and second layers, and its maximum amplitude acually occurs in the first layer. (As a result, S_1 also lies below the first-layer mode S_3.) According to the above interpretation of the surface modes, at $\overline{Y}$ one would expect S_1 to be a second-layer SV-like mode and S_5 to be a first-layer P-like mode. In fact, each has a mixture of these two characters. It is as if S_1 and S_5 were in some sense hybridizing near $\overline{Y}$—i.e., as if S_1 were trying to assume a second-layer SV character upon approaching $\overline{Y}$ and S_5 were trying

to assume a first-layer longitudinal character. The behavior of S_1 on the right-hand side of Fig. 13 is the only feature of our calculated surface-mode spectra that does not fit very well into the simple model of this section.

There are three cases in the present results in which surface modes attempt to cross each other, and as a consequence clearly exhibit hybridization: S_1 and S_4 in Fig. 10, to the right of X; S_1 and S_2 in Fig. 13, to the left of $\bar{S}$; and S_2 and S_3 in Fig. 13, to the left of $\bar{Y}$.

It should be mentioned that the "peeling-off" description discussed here is also applicable, with modifications, to other types of surface states besides surface phonons. Discussions of surface magnons,[25] surface plasmons,[26] and surface electronic states[27] have recently appeared. In one of the models of Ref. 25, it was found that a second-layer surface magnon branch appeared in addition to the first-layer branch if the surface exchange parameters were softened. There is an obvious analogy with S_2 in Fig. 10 of the present paper, which is a second-layer surface phonon branch (and which appears only when the surface force constants are softened; see Sec. VI). In Ref. 25, it was found that surface magnon branches could be peeled off the top of the continuum of bulk magnons if the exchange parameters were stiffened, just as Musser and Rieder[24] found surface phonon branches to be peeled off the top of the bulk phonon bands when the surface force constants were stiffened. In the model of Ref. 26, a series of surface plasmons was peeled off the continuum of bulk plasmons as the extent of the surface region was increased; up to three surface plasmon branches were found. In the model of Ref. 27, up to six surface electronic states were obtained near the edge of the BZ as the geometry of the surface region was perturbed.

In the case of all four types of states—phonons, magnons, plasmons, and single-electron states—the perturbation represented by the surface can peel off a series of surface states from the bulk band or bands. This perturbation consists of two parts: The "first-order" perturbation is simply the truncation of the crystal by the surface. The "second-order" perturbation is a change in the surface force constants (for phonons), a change in the surface exchange parameters (for magnons), or a change in the surface geometry and electronic structure (for plasmons and electronic states.)

VI. EFFECT OF CHANGES IN DENSITY AND SURFACE FORCE CONSTANTS

It is of some interest to determine how the surface modes are affected by changes in the crystal density or in the force constants near the surface.[28] In Fig. 18, the dispersion curves are shown for a density corresponding to $\sigma/a = 1.24$. (Since σ is to be regarded as fixed, a reduction in the ratio σ/a corresponds to an increase in a or an expansion of the crystal.) This value of σ/a represents (approximately) the correct density near the melting point, whereas $\sigma/a = 1.297$ represents the correct density for a static crystal.[29] The results of Fig. 10 and Fig. 18, therefore, correspond to the extreme limits of the crystal density. Notice that there is virtually no difference in the qualitative features of Figs. 10 and 18: The surface-mode spectra are the same, except that the (marginal) surface mode S_{11} has become a mixed mode MS_{11}, and the surface-mode frequencies have been diminished in proportion to the bulk-mode frequencies. We thus have the result that the Grüneisen parameters for the surface modes are very nearly equal to those for the bulk modes. The same result is obtained in calculations for the (111) and (110) surfaces.

One word of caution is necessary, however: Although the Grüneisen parameters for surface and bulk modes are approximately equal, the surface region and bulk region will not actually expand by the same amount as we have assumed in obtaining the results of Fig. 18. Ordinarily, there should be a large degree of thermal expansion near the surface.[4] This differential thermal expansion should have the effect of strengthening the perturbation associated with the surface and should produce two effects: (a) The surface-mode frequencies should show a decrease relative to the bulk-mode frequencies as the crystal expands. (b) In some cases, new surface modes should appear (or drop down into bulk bands and disappear) as the crystal expands. If detailed experimental studies of high-frequency surface modes become possible, it would be interesting to test these conclusions.

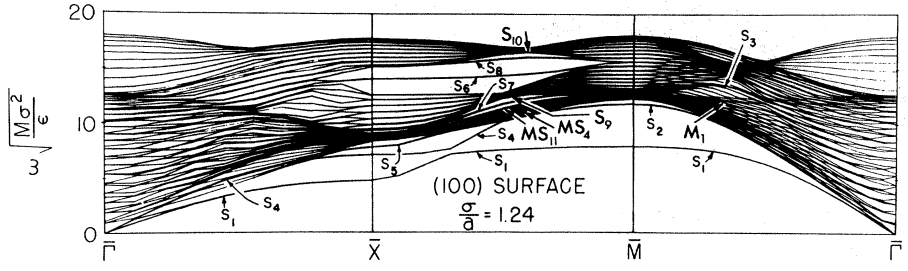

FIG. 18. ω vs $\bar{q}$ for (100) surface at a crystal density corresponding to $\sigma/a = 1.24$, where $\sqrt{2}\,a$ is the nearest-neighbor distance in the bulk.

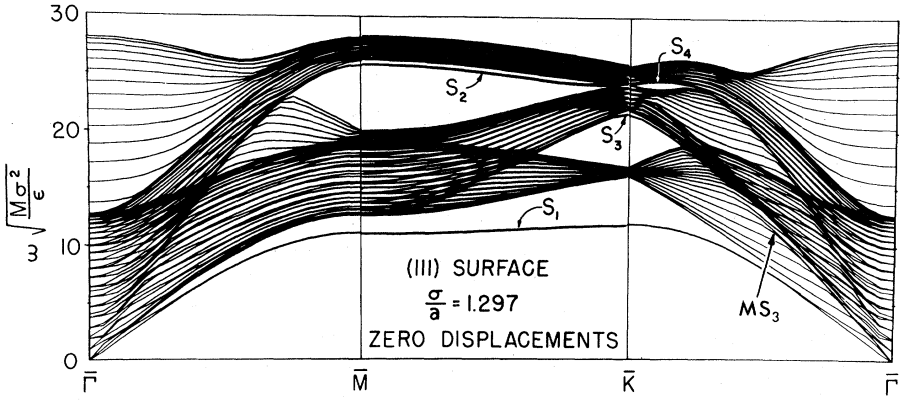

FIG. 19. ω vs $\bar{q}$ for (111) surface without surface relaxation taken into account; i.e., the interplanar spacings are the same near the surface as in the bulk of the crystal.

Now we turn to the effect of changes in the surface force constants with the crystal density held fixed. In Figs. 19–21, the frequency spectra are shown for the (111), (100), and (110) surfaces with the static displacements set equal to zero; i.e., the relaxation of the surface particles is not taken into account, so that the interplanar spacing is the same throughout the crystal. When the relaxation is turned off, the surface force constants are increased to their bulk values and the surface-mode frequencies are consequently also increased. In some cases the surface modes are raised into the bulk and cease to exist as surface modes.

The effect of turning off the relaxation is smallest for the (111) surface since the magnitude of the relaxation is smallest for the surface (see Fig. 2 of Ref. 4). All of the surface-mode frequencies are raised somewhat, but only S_5 is completely destroyed.

For the (100) surface, the frequencies are raised by a larger amount, and S_2 is completely destroyed. The modes S_5 and S_8 are destroyed everywhere except in a tiny region under the bottlenecks in the lowest and highest bulk bands, respectively, as indicated in Fig. 20. In addition the modes above S_5 at $\bar{X}$, above S_7 at the bottleneck in the middle subband (including S_9), and above S_8 in the highest subband (including S_{10}) have been destroyed.

For the (110) surface, the surface-mode frequencies have again been considerably increased. Near $\bar{X}$, along $\bar{X}\bar{S}$, S_2 has been raised into the lowest subband to become a mixed mode MS_2. At $\bar{Y}$, S_4 and S_9 have been completely destroyed, and so has S_{10} at $\bar{X}$. It appears that S_6 and S_8 have also been completely destroyed, even under the bottlenecks in the highest bulk band. As indicated in Fig. 21, at some points these surface modes persist as mixed modes MS_6 and MS_8. In Fig. 22(b), we graph the squared amplitudes of MS_2, MS_6, and MS_8 at the points indicated by the arrows in Fig. 21. In Fig. 22(a), we graph S_2, S_6, and S_8 of Fig. 13 at these same points. It is evident that MS_2, MS_6, and MS_8 are, in fact, mixed modes.

The substantial changes in the surface-mode spectra that result from neglecting the surface relaxation are not surprising in view of the large changes in the surface force constants that are produced by this relaxation. The change in the interplanar spacing at the surface due to relaxation is 1.2, 2.6, and 3.7% for the (111), (100), and (110) surfaces, respectively.[4] This change is to be compared with the 4–5% change which results in the bulk from thermal expansion between 0 °K ($\sigma/a \approx 1.30$) and the melting temperature ($\sigma/a \approx 1.24$).

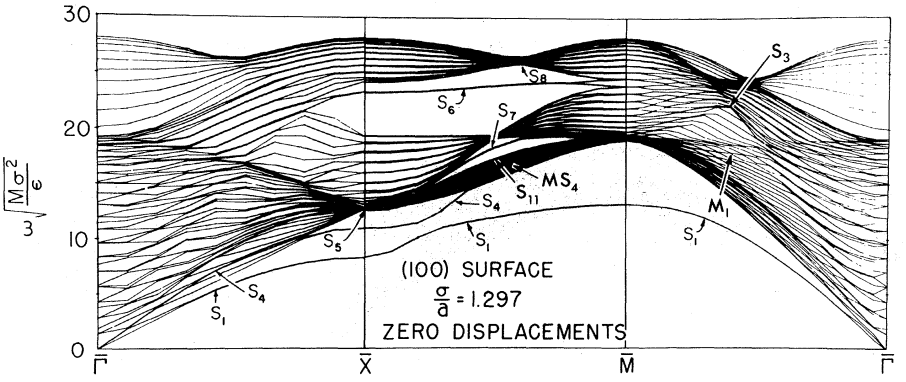

FIG. 20. ω vs $\bar{q}$ for (100) surface without surface relaxation taken into account.

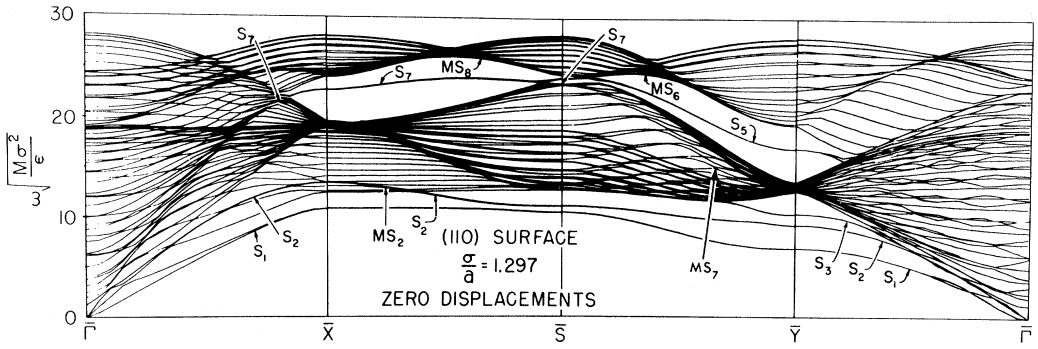

FIG. 21. ω vs $\bar{q}$ for (110) surface without surface relaxation taken into account.

As can be seen from a comparison of Figs. 10 and 18, the bulk vibrational frequencies (in the quasiharmonic approximation) are reduced by about a third as a result of this 4–5% expansion. It is therefore to be expected that the expansion near the surface of a few percent, due to relaxation, will have a profound effect on the surface modes.

It should be mentioned that Musser and Rieder[24] have examined the effect of changes in the surface force constants on the surface-mode frequencies for the line $\bar{\Gamma}\bar{M}$ in the case of the (100) surface. Their calculations were based on a force-constant model with parameters appropriate to nickel. Their surface-mode spectrum for this direction and surface are in excellent agreement with those of the present paper (right-hand sides of Figs. 10 and 20), which have been previously given in Ref. 3. In addition, they find the same general behavior of S_1, S_2, and S_3 with respect to changes in the surface force constants as was described above (increase in frequency of S_1, complete extinction of S_2, near extinction of S_3 when the surface force constants are assumed to be equal to those in bulk).

Musser and Rieder also find a surface-mode branch below S_3 which apparently corresponds to our mixed mode M_1 (first-layer analog of S_3). This surface-mode branch is not very prominent, however. We do not find it in our results, possibly because of the difference between our model and theirs. When the surface force constants are stiffened, this surface-mode branch rises up out of the lowest bulk band to become more prominent. Another surface-mode branch is peeled off the top of this lowest band, and there is evidently hybridization when the two surface-mode branches attempt to cross (see the inset in Fig. 2 of Ref. 24).

It is remarkable that the results of Musser and Rieder, which are for a model of nickel with noncentral forces and the surface force constants adjusted to agree with experimental data, are in very close agreement with the results of the present paper and Ref. 3, which were obtained from first principles for a Lennard-Jones potential.

VII. FREQUENCY DISTRIBUTION FUNCTIONS

In this section we consider the effect of the surface modes on the frequency distribution function $f(\omega)$, which is defined such that $f(\omega)\,d\omega$ is the frac-

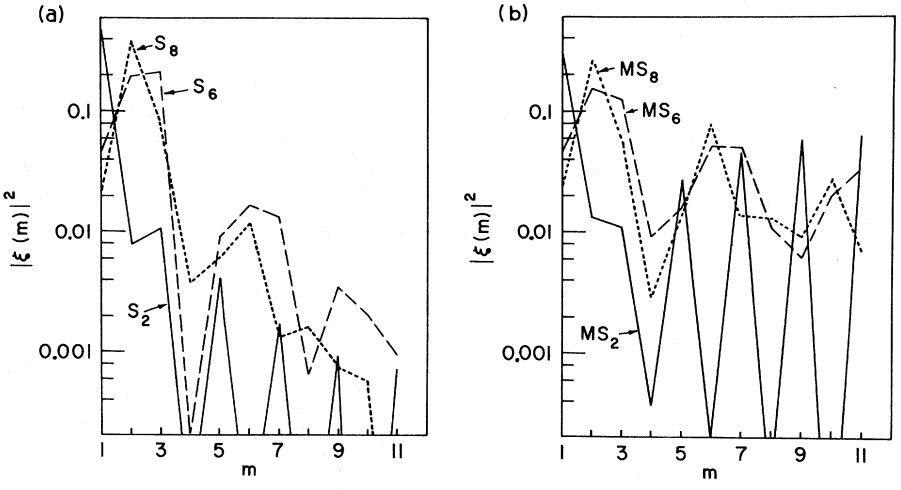

FIG. 22. Graph of squared amplitude vs distance from surface for the mixed modes MS_2, MS_6, and MS_8 at the positions indicated by the arrows in Fig. 21. The surface modes S_2, S_6, and S_8 for the (110) surface with relaxation taken into account (results of Fig. 13) are graphed at these same points.

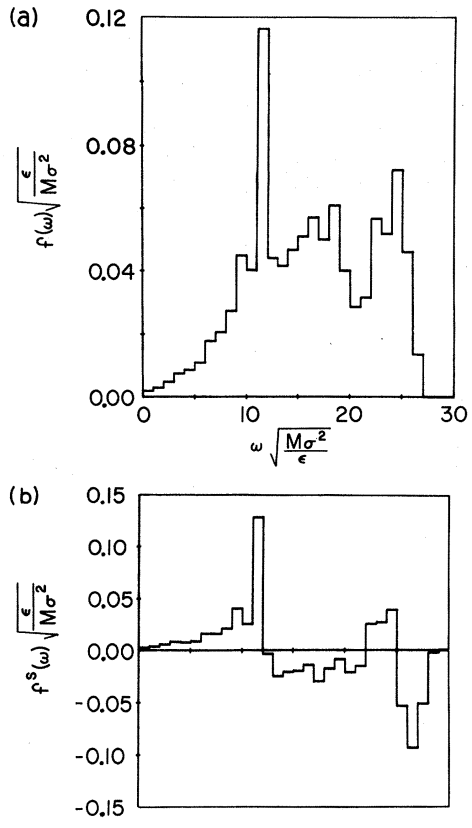

FIG. 23. Frequency distribution function $f(\omega)$ and surface frequency distribution function $f^s(\omega)$ for three-layer crystal with (111) surfaces.

tion of the frequencies lying between ω and $(\omega + d\omega)$. In Fig. 23(a), the dimensionless quantity $(\epsilon/M\sigma^2)^{1/2} f(\omega)$ is shown for a three-layer crystal with (111) surfaces.[30] [The corresponding dispersion curves are shown in Fig. 2(a).] In Fig. 23(b), the surface frequency distribution function $f^s(\omega)$ is shown. This function is defined as the difference between $f(\omega)$ and the frequency distribution function for the bulk, $f^b(\omega)$, multiplied by an appropriate normalization factor[31]:

$$f^s(\omega) = (N/N_s)[f(\omega) - f^b(\omega)] .$$

Here N_s is the number of surface particles and N the total number of particles in the crystal with surfaces.

The peak in $f^s(\omega)$ at low frequencies is, of course, caused by the presence of the low-frequency surface mode (S_1 in Fig. 8). The peak at high frequencies is caused by the "gap" surface modes (S_2, S_3, and S_4 in Fig. 8). Since the surface modes are in effect pulled out of the bulk bands, there must be a depletion in these bands. This depletion shows up in the negative values of $f^s(\omega)$ that can be observed in Fig. 23(b).

It may be worth mentioning that $f^s(\omega)$ can have discontinuities and logarithmic singularities, as opposed to the frequency distribution function for the bulk, which is continuous and has singularities in its derivative only.[32] The presence of singularities in $f^s(\omega)$ is suggested by the histograms of Fig. 23(b).

In Ref. 31, the values of $f(\omega)$ and $f^s(\omega)$ are given for thicker crystals. It is interesting that the qualitative features do not change in going from a three-layer crystal to a much thicker one. The main change is that the peak associated with the lowest-frequency surface mode becomes less steep, since its dispersion curve becomes less flat near the edge of the BZ.

Another quantity that is of some interest is what we call the "effective frequency distribution function," $f_\alpha(\omega; l_3)$, for the α direction ($\alpha = x, y, z$) and the l_3th layer. We define this function by the equation[33]

$$f_\alpha(\omega; l_3)\, d\omega = \frac{1}{\overline{N}} \sum_{\omega \le \omega' \le \omega + d\omega} |\xi_\alpha(l_3; \omega')|^2 , \qquad (7.1)$$

where $\xi_\alpha(l_3; \omega)$ is the (α, l_3) component of the eigenvector associated with the normal mode having frequency ω and $\overline{N}$ is the number of particles per layer. The contribution of a frequency to $f_\alpha(\omega; l_3)$ is thus weighted according to the amplitude of the corresponding mode in the α direction and the l_3th layer. The mean-square amplitude of vibration $\langle u_\alpha^2(l_3)\rangle$ can be expressed in terms of $f_\alpha(\omega; l_3)$ as follows:

$$\langle u_\alpha^2(l_3)\rangle = \frac{\hbar}{2\overline{N}M} \sum_\omega |\xi_\alpha(l_3; \omega)|^2 \frac{\coth(\hbar\omega/2k_B T)}{\omega} \qquad (7.2)$$

$$= \frac{\hbar}{2M} \int_0^{\omega_{\max}} \frac{\coth(\hbar\omega/2k_B T)}{\omega} f_\alpha(\omega; l_3)\, d\omega , \qquad (7.3)$$

where k_B is the Boltzmann constant, M the mass of a particle, T the temperature, and $\omega_{\max}$ the maximum vibrational frequency.

In Fig. 24, the values of $f_\alpha(\omega; l_3)$ for l_3 corresponding to the surface layer are given for the (111), (100), and (110) surfaces. [We leave out the index l_3 and write $f_\alpha(\omega)$ when referring to the surface layer. The results of Fig. 24 were obtained with 21-layer crystals.] $f_x(\omega)$ is rather flat and not much different from the bulk $f(\omega)$ for all three surfaces. [For the (111) and (100) surfaces, $f_y(\omega) = f_x(\omega)$.] $f_z(\omega)$ is large at low frequencies because of the presence of low-frequency surface modes associated with this direction of vibration. In the case of the (110) surface, there are also prominent low-frequency surface modes associated with the y direction (S_2 on the left side of Fig. 13 and S_1 on the right side, after the interchange of character).

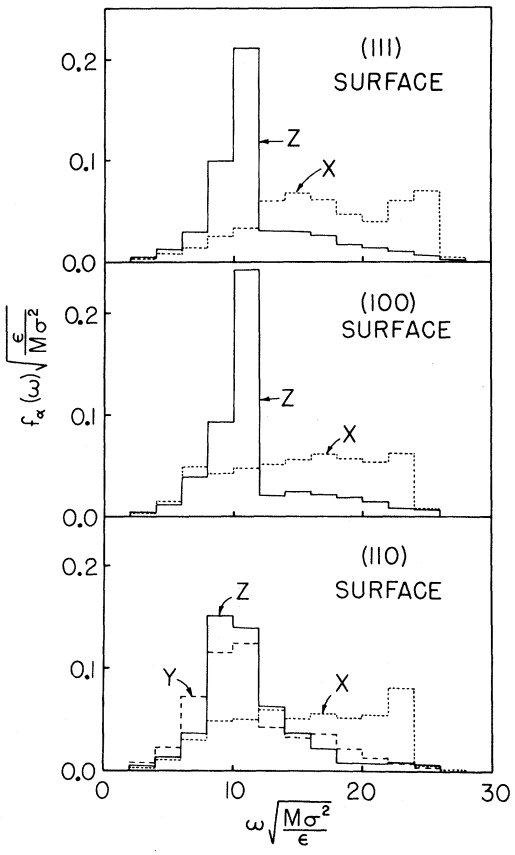

FIG. 24. Effective frequency distribution functions at surface, $f_\alpha(\omega)$ ($\alpha = x, y, z$), for (111), (100), and (110) surfaces. These results were obtained with 21-layer crystal at a crystal density corresponding to $\sigma/a = 1.297$.

One can calculate a similar "effective frequency distribution function" using molecular dynamics[34]—i.e., by performing a computer experiment with the particles taken to obey classical equations of motion. In this case we define $f_\alpha(\omega; l_3)$ to be a Fourier transform of the velocity autocorrelation function for the α direction and l_3th layer:

$$f_\alpha(\omega; l_3) = \int_0^\infty \frac{\langle v_\alpha(\vec{l}; t+t_0) v_\alpha(\vec{l}; t_0)\rangle_{l_3}}{\langle v_\alpha(\vec{l}; t_0) v_\alpha(\vec{l}; t_0)\rangle_{l_3}} \cos\omega t \, dt \,, \tag{7.4}$$

where $v_\alpha(\vec{l}; t)$ is the α component of the velocity of the particle with index $\vec{l}$ at time t. The angular brackets indicate an average over the l_3th layer only, and t_0 is an arbitrary initial time.

In Fig. 25 some molecular-dynamics results for $f_\alpha(\omega; l_3)$ at the surface are shown, together with the similarly defined $f(\omega)$ for the whole crystal. The statistics are not very good, especially for the averages over only a single layer, but the peaks in $f_\alpha(\omega)$ occur at about the same place as they do in the results obtained with lattice dynamics at this density.

VIII. CONCLUSIONS

Until the present work (including Refs. 2 and 3), the only vibrational surface modes known to exist in monatomic crystals were the generalized Rayleigh waves which are obtained in the continuum approximation.[10] These waves lie beneath the bulk subbands (except possibly along certain symmetry directions), and their attenuation with distance from the surface is rather simple as indicated in Eq. (1.2) of I.

In the present work it has been found that there are, in addition to the generalized Rayleigh waves, other surface modes which are characterized by the fact that they do not persist into the long-wavelength limit and therefore cannot be obtained in the continuum approximation. The dependence of the amplitude of these modes upon the distance from the surface is generally rather complex.

The main qualitative findings of the present paper are the following: (a) The surface phonon spectrum is remarkably complex even for monatomic crystals with low-index surfaces. (b) There can be gaps within the subbands corresponding to acoustic bulk modes, as shown in the bottom part of Fig. 7. (There can also be gaps within the subbands for optical bulk modes[12] and, for some materials, gaps between the subbands for optical bulk modes and those for acoustic bulk modes.) High-frequency surface modes can be, and usually are, present within these gaps. (c) It is possible for surface modes to exist within the bulk subbands for propagation vectors $\bar{q} = (q_x, q_y)$ which lie along certain symmetry directions in the two-dimensional BZ, and such surface modes are a commonplace occurrence. Surface modes within the bulk continua are also possible at other exceptional points in the BZ, such as the point $\bar{S}$ in Fig. 1. Whatever surface modes exist within the bulk continua along such a symmetry line, or at such a symmetry point, will degenerate into mixed modes for $\bar{q}$ slightly removed from the line or point. (d) There can be surface modes which are primarily localized in some plane of particles beneath the surface, rather than in the surface plane itself, and such modes are, in fact, commonplace. (e) The attenuation of surface modes with distance from the surface is generally rather complex. The magnitude $|\vec{\xi}(l_3)|^2$ need not fall off monotonically, or even regularly. (f) The qualitative features of the surface phonon spectrum are sensitive to changes in the surface force constants. In the model which we have used for calculations, if the static relaxation is "turned off," then some surface modes are raised into the bulk continua and are no longer completely localized. This fact implies that a correct prediction of the surface-mode spectrum must be based upon an accurate knowledge of the force constants at the surface. However, the

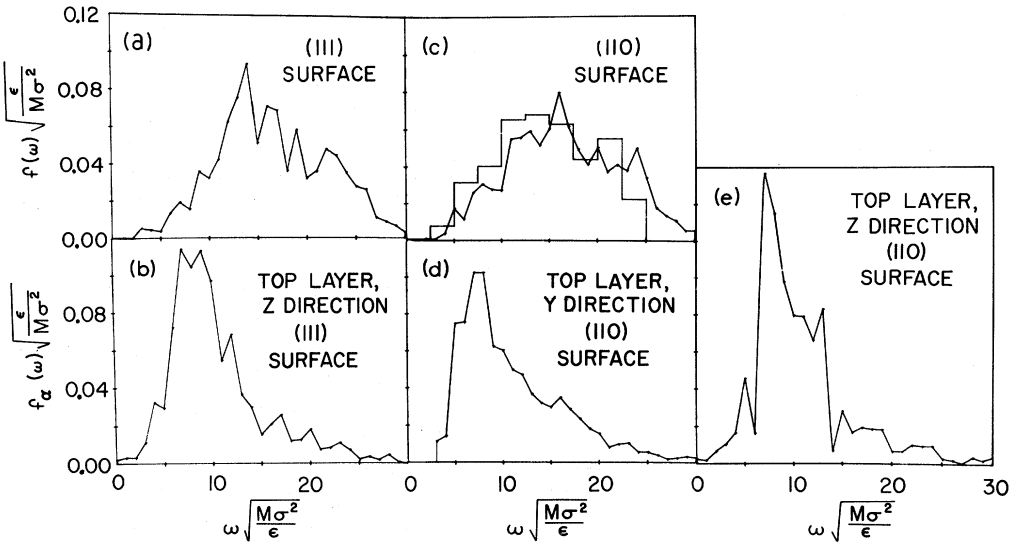

FIG. 25. Frequency distribution functions $f(\omega)$ and effective frequency distribution functions at surface, $f_\alpha(\omega)$, calculated in molecular dynamics computer experiments. (a) $f(\omega)$ for 11-layer crystal with (111) surfaces. (b) $f_z(\omega)$ for (111) surface. (c) $f(\omega)$ for 11-layer crystal with (110) surfaces. The histogram was calculated for the same model using lattice dynamics rather than molecular dynamics. (d) $f_y(\omega)$ for (110) surface. (e) $f_z(\omega)$ for (110) surface. All of these results were obtained with 11-layer crystals at a density corresponding to $\sigma/a = 1.28$. The temperatures were given by $k_BT/\epsilon = 0.369$ for (a) and (b), and by $k_BT/\epsilon = 0.335$ for (c), (d), and (e).

qualitative features of the surface-mode spectrum are not appreciably affected by uniform changes in density, which cause the surface force constants to change approximately in proportion to those of the bulk. (g) Despite the complexity of the surface-mode spectra, all of the surface modes and mixed modes found can be described in terms of a very simple phenomenological model. In this model, the surface is regarded as a perturbation which "peels off" surface and mixed modes from the bulk bands. The number of modes peeled off depends on the strength of the perturbation for a particular wave vector $\bar{q}$. From a given bulk band, the modes are peeled off in a series of like character, with a first-layer mode peeled off first, then a second-layer mode, etc.

The calculations of this paper were performed for model crystals in which the particles interact through a Lennard-Jones potential. However, it is reasonable to expect that many of the qualitative findings will be of general validity. This expectation is strengthened by the rough agreement of our results at long wavelengths with those of Farnell[10] and of Lim and Farnell,[21,22] which were obtained in the continuum approximation for materials such as Ge, KCl, and Si. Further support is provided by the calculations for a discrete lattice model of NaCl,[12] which is, of course, quite different from the present model in having long-range Coulomb forces and two particles per primitive unit cell, and by calculations for a model of Ni with noncentral forces in which the surface force constants were adjusted to experimental data.[24]

To our knowledge, there is as yet no experimental evidence for the existence of the new surface modes found here, which are present only at short wavelengths. (The possibility of their existence was, however, pointed out for the first time in Ref. 2.) In principle these surface modes and similar modes which have subsequently been found in calculations for an ionic crystal[12] should be detectable in neutron-,[35] electron-,[36] or atomic-[37] scattering experiments.

---

*Research sponsored by the Air Force Office of Scientific Research, Office of Aerospace Research, U. S. Air Force under Grant Nos. AFOSR-71-1973 and AFOSR-1257-67.

†Present address: Department of Physics, Texas A&M University, College Station, Tex. 77843.

[1(a)]R. E. Allen, G. P. Alldredge, and F. W. de Wette, preceding paper, Phys. Rev. B 4, 1648 (1971). We will refer to this paper as I; (b) G. P. Alldredge, R. E. Allen, and F. E. de Wette, following paper, Phys. Rev. B 4, 1682 (1971).

[2]R. E. Allen, G. P. Alldredge, and F. W. de Wette, Phys. Rev. Letters 23, 1285 (1969).

[3]R. E. Allen, G. P. Alldredge, and F. W. de Wette, Phys. Rev. Letters 24, 301 (1970).

[4]R. E. Allen and F. W. de Wette, Phys. Rev. 179, 873 (1969).

[5]As defined in I, a "subband" is a range of allowed fre-

quencies for a particular set of modes at a fixed value of the two-dimensional propagation vector $\bar{q} = (q_x, q_y)$.

[6]The small value of the slope of the lowest branch near $\bar{\Gamma}$ is due to the small restoring force for long-wavelength flexing of a very thin plate. As more layers are added, the plate becomes stiffer and the slope becomes larger, as one can observe in Figs. 3 and 8.

[7]This point of view has been adopted by A. A. Maradudin and J. Melngailis [Phys. Rev. 133, A1188 (1964)] in conjunction with a Green's-function approach.

[8]There are also minor differences between the results of Figs. 7 and 8 which are due to the fact that no attempt was made to connect the curves properly in the event of crossovers (see the caption to Fig. 3).

[9]We label the surface modes by arbitrarily assigning a number to each pair of surface-mode branches in the slab. (As mentioned in Sec. II and in Ref. 1, there are two nearly degenerate surface modes of each kind in a slab, which correspond to a single surface mode in a semi-infinite crystal.) A series of mixed modes which is related to the branch S_i of surface modes is labeled by MS_i.

[10]G. W. Farnell, in *Physical Acoustics*, edited by W. P. Mason and R. N. Thurston (Academic, New York, 1970), Vol. 6.

[11]G. P. Alldredge, R. E. Allen, and F. W. de Wette, J. Acoust. Soc. Am. 49, 1453 (1971).

[12]T. S. Chen, R. E. Allen, G. P. Alldredge, and F. W. de Wette, Solid State Commun. 8, 2105 (1970). In this model of NaCl, there are gaps between the bulk subbands for both acoustical and optical modes. S. Y. Tong and A. A. Maradudin [Phys. Rev. 181, 1318 (1969)] also studied the surface-mode spectrum of the same model, but did not point out the surface modes that occur in these gaps between bulk subbands.

[13]According to the general result in Sec. III B of I, any mode associated with a wave vector $\bar{q}$ lying along the line $\bar{\Gamma}\,\bar{M}$ must either be strictly an SH mode or else be polarized strictly in the sagittal plane—i.e., the plane containing $\bar{q}$ and the normal to the surface. Therefore, along $\bar{\Gamma}\,\bar{M}$, S_1 and S_2 are polarized strictly within the sagittal plane.

[14]The frequencies and eigenvectors were recalculated for a number of finely spaced points in the region of closest approach, in order to make certain that S_1 and S_4 do not cross.

[15]See, e.g., W. A. Harrison, *Solid State Theory* (McGraw-Hill, New York, 1970), pp. 204–205.

[16]One can show that the following is true for any point lying on the edge of the BZ ($\bar{X}\,\bar{M}$) in the case of the (100) surface: either $\xi_x(m) = \xi_y(m)$ and $\xi_z(m) = 0$, or else $\xi_x(m) = -\xi_y(m)$; if one statement holds for even m, the other holds for odd m.

[17]The x, y, and z axes are defined in Fig. 1 of Ref. 34. In Fig. 1 of the present paper, the x axis is in the horizontal direction and the y axis in the vertical direction. For the (100) surface, therefore, the x axis is in the same direction as the line $\bar{\Gamma}\,\bar{M}$, and the y axis is perpendicular to $\bar{\Gamma}\,\bar{M}$. For the (110) surface, the x and y axis, respectively, point in the directions of $\bar{\Gamma}\,\bar{X}$ and $\bar{\Gamma}\,\bar{Y}$. The z axis is always normal to the surface.

[18]The fact that only one bulk mode lies under S_2 in Fig. 13 may raise a slight doubt as to whether S_2 would actually lie within the bulk "bands" in a very thick crystal. We have therefore repeated the calculation for some points along the line $\bar{\Gamma}\,\bar{X}$ using a 31-layer crystal, and it is found that in the thicker crystal there are more bulk bands under S_2 and that the frequencies associated with S_2 are virtually unchanged. We have performed a similar check for S_4 in Fig. 10.

[19]S_7 is polarized strictly parallel to the surface at $\bar{S}$, and the modes surrounding it are polarized strictly normal to the surface.

[20]The fact that some of the attenuation graphs in Figs. 14 and 15 show a sudden upturn at $m = 11$ (the center layer) is due to the finite thickness of the crystal. As shown in I, the surface modes in our slab-shaped model occur in pairs. In the present paper, we have ordinarily plotted the member of the pair which has the larger amplitude at the center.

[21]T. C. Lim and G. W. Farnell, J. Appl. Phys. 39, 4319 (1968).

[22]T. C. Lim and G. W. Farnell, J. Acoust. Soc. Am. 45, 845 (1969).

[23]It is interesting, however, that the hybridization still occurs near the edge of the Brillouin zone in the results for the rigid-ion model of NaCl used in Ref. 12; see T. S. Chen, G. P. Alldredge, F. W. de Wette, and R. E. Allen, Phys. Rev. Letters 26, 1543 (1971), Fig. 2. For NaCl, which has $\eta < 1$, one indeed finds that the SH branch lies above the SV branch along $\bar{\Gamma}\,\bar{X}$ at large wavelengths. However, as the BZ edge is approached along $\bar{\Gamma}\,\bar{X}$, the SH and SV branches *cross* and along the zone edge the SV branch lies higher (where it is, in fact, a mixed mode buried in the lowest bulk band), so that there is still hybridization along the zone edge. As a result, the lowest surface-mode branch changes polarization, from SH to primarily SV, between $\bar{X}$ and $\bar{M}$, just as it does for our model in Fig. 10.

[24]S. W. Musser and K. H. Rieder, Phys. Rev. B 2, 3034 (1970).

[25]R. E. De Wames and T. Wolfram, Phys. Rev. 185, 720 (1969); 185, 752 (1969); T. Wolfram and R. E. De Wames, *ibid.* 185, 762 (1969).

[26]A. J. Bennett, Phys. Rev. B 1, 203 (1970).

[27]J. D. Levine and S. Freeman, Phys. Rev. B 2, 3255 (1970).

[28]The principal results of this section have been previously reported by R. E. Allen, G. P. Alldredge, and F. W. de Wette [Bull, Am. Phys. Soc. 15, 101 (1970)].

[29]We assume that the crystal is not under pressure and that a Lennard-Jones potential is appropriate.

[30]The histograms in Figs. 23 and 24 and the straight line graph in Fig. 25 are only approximations to the actual (smooth) distribution, of course.

[31]R. E. Allen and F. W. de Wette, J. Chem. Phys. 51, 4820 (1969).

[32]L. Van Hove, Phys. Rev. 89, 1189 (1953); Ya. A. Iosilevskii, Zh. Eksperim. i Teor. Fiz. Pis'ma Redaktsiya 7, 32 (1968) [Sov. Phys. JETP Letters 7, 22 (1968)].

[33]R. E. Allen, G. P. Alldredge, and F. W. de Wette, Phys. Rev. B 2, 2570 (1970).

[34]R. E. Allen, F. W. de Wette, and A. Rahman, Phys. Rev. 179, 887 (1969).

[35]K. H. Rieder and E. M. Hörl, Phys. Rev. Letters 20, 209 (1968).

[36]H. Ibach, Phys. Rev. Letters 24, 1416 (1970).

[37]N. Cabrera, V. Celli, and R. Manson, Phys. Rev. Letters 22, 346 (1969); R. Manson and V. Celli, Surface Sci. 24, 495 (1971).